Accepted Manuscript

Design, synthesis, topoisomerase I & II inhibitory activity, antiproliferative activity, and structure-activity relationship study of pyrazoline derivatives: An ATP-competitive human topoisomerase IIα catalytic inhibitor

Pervez Ahmad, Hyunjung Woo, Kyu-Yeon Jun, Adnan A. Kadi, Hatem A. Abdel-Aziz, Youngjoo Kwon, A.F.M. Motiur Rahman

PII: S0968-0896(16)30166-3
DOI: http://dx.doi.org/10.1016/j.bmc.2016.03.017
Reference: BMC 12866

To appear in: *Bioorganic & Medicinal Chemistry*

Received Date: 10 February 2016
Revised Date: 7 March 2016
Accepted Date: 8 March 2016

Please cite this article as: Ahmad, P., Woo, H., Jun, K-Y., Kadi, A.A., Abdel-Aziz, H.A., Kwon, Y., Motiur Rahman, A.F.M., Design, synthesis, topoisomerase I & II inhibitory activity, antiproliferative activity, and structure-activity relationship study of pyrazoline derivatives: An ATP-competitive human topoisomerase IIα catalytic inhibitor, *Bioorganic & Medicinal Chemistry* (2016), doi: http://dx.doi.org/10.1016/j.bmc.2016.03.017

Design, synthesis, topoisomerase I & II inhibitory activity, antiproliferative activity, and structure-activity relationship study of pyrazoline derivatives: an ATP-competitive human topoisomerase IIα catalytic inhibitor

Pervez Ahmad,[a,#] Hyunjung Woo,[b,#] Kyu-Yeon Jun,[b] Adnan A. Kadi,[a] Hatem A. Abdel-Aziz,[a,c] Youngjoo Kwon,[b,*] A. F. M. Motiur Rahman[a,*]

[a]*Department of Pharmaceutical Chemistry, College of Pharmacy, King Saud University, Riyadh 11451, Saudi Arabia;* [b]*College of Pharmacy, Graduate School of Pharmaceutical Sciences, Ewha Womans University, Seoul, 120-750, Republic of Korea. Department of Applied Organic Chemistry Department, National Research Center, Dokki, Cairo 12622, Egypt.*

*Corresponding Authors: Tel: +82232774653, fax: +82232772851, email: ykwon@ewha.ac.kr (Y. Kwon) Tel: +966114670237, fax: +966114676220, email: afmrahman@ksu.edu.sa (A. F. M. Motiur Rahman)

#Authors are equal contributor

Abstract

A series of pyrazoline derivatives (**5**) were synthesized in 92-96 % yields from chalcones (**3**) and hydrazides (**4**). Subsequently, topo-I and IIα-mediated relaxation and antiproliferative activity assays were evaluated for **5**. Among the tested compounds, **5h** had a very strong topo-I activity of 97% (camptothecin, 74%) at concentration of 100μM. Nevertheless, all the compounds **5a-5i** showed significant topo II inhibitory activity in the range of 90-94% (Etoposide, 96%) at the same concentration. Cytotoxic potential of these compounds was tested in a panel of three human tumor cell lines, HCT15, BT474 and T47D. All the compounds showed strong activity against HCT15 cell line with IC_{50} at the range of 1.9-10.4 μM (Adriamycin, 23.0; Etoposide, 6.9; and Camptothecin, 7.1 μM). Moreover, compounds **5c**, **5f** and **5i** were observed to have strong antiproliferative activity against BT474 cell lines. Since, compound **5d** showed antiproliferative activity at a very low IC_{50} thus **5d** was then selected to study on their mode of action with diverse methods of ATP competition assay, ATPase assay and DNA-topo IIα cleavable complex assay and the results revealed that it functioned as a ATP-competitive human topoisomerase IIα catalytic inhibitor. Further evaluation of endogenous topo-mediated DNA relaxation in cells has been conducted to find that, **5d** inhibited endogenous topo-mediated pBR322 plasmid relaxation is more efficient (78.0 ± 4.7% at 50 μM) than Etoposide (36.0 ± 1.7 % at 50 μM).

Keywords

Pyrazoline derivatives; Antiproliferative activity; Topoisomerase; ATP-Competitive Inhibitor;

Introduction

Pyrazolines have shown a variety of biological properties [1-41] including antitumor activity [21, 22, 33], anticancer activity on colon cancers cell line [42]. Recently, pyrazoline-based selective fluorescent probe for detecting reduced glutathione and its application in living cells and serum has been reported [43]. It should be noted that, number of drugs are in market containing pyrazole/pyrazoline/pyrazolidine moieties have been used for various treatments, e.g. Celecoxib [44], Famprofazone [45], Deracoxib [46], Sulfinpyrazone [47], Apixaban [48], Allopurinol [49], Rimonabant [50], Ruxolitinib [51], Sulfaphenazole [52], and Phenazone [53]. In addition, some of the derivatives are under pre-clinical studies, e.g. SLV-330 [54, 55] and E-6087 [56, 57] (Chart 1). However, neither systematic SAR studies nor mechanistic studies have not been pursues as yet.

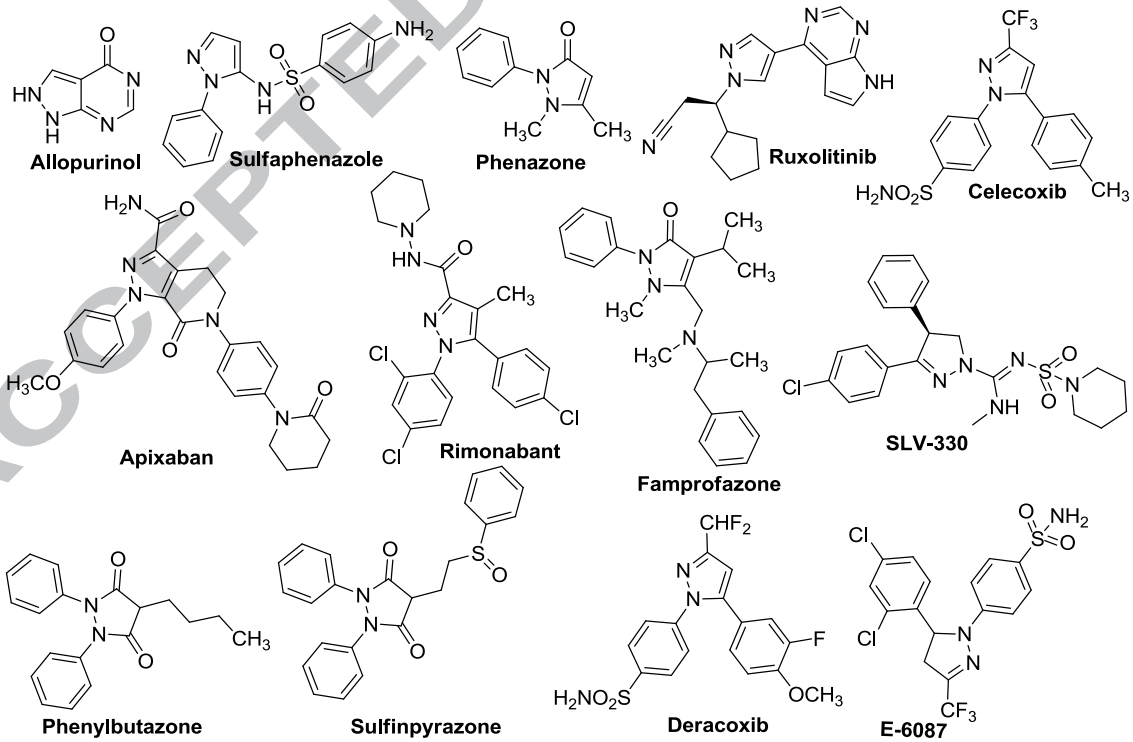

Chart 1. Structures of some drugs containing pyrazole / pyrazoline / pyrazol-3-ones / pyrazoline-3,5-dione moiety

Though numbers of pyrazoline derivatives have been reported with various biological activities, and a numbers of drugs are currently available in market with pyrazole/pyrazoline/pyrazolidine moieties, their intriguing structures and various biological activities attracting the attention of researcher to synthesize novel pyrazoline derivatives for the development of potential anticancer therapeutics. Since, DNA is one of the most important pharmacological targets of many drugs. DNA topoisomerases are enzymes that transiently break one or two strands of DNA, which allow to solve various DNA topological problems generated during vital cellular processes [58-67]. Because of the crucial role of topoisomerases for the maintenance and replication of DNA during proliferation, topoisomerase inhibitors are among the most potent anticancer agents to date. Our research group has been focusing on development of human topo IIα catalytic inhibitors [58-62] especially using chalcone moiety [63-66], to enhance topo IIα catalytic inhibitory activity. As part of our broad interest finding novel topo inhibitors, we have designed and synthesized a series of novel pyrazoline derivatives, derived from various chalcones and substituted 2-carbohydrazide, evaluated their cytotoxic potential against various human cancer cell lines, topo I & II inhibitory activities by assessing the relaxation of supercoiled pBR 322 plasmid DNA, evaluated mode of action of the most active compound by performing DNA-topo cleavage complex, topo IIα-mediated ATP competition assay and ATPase assay, studied molecular docking, and evaluated the effect of compound on cell by endogenous topo inhibition assay for the development of new anticancer therapeutics.

Results and discussion

Chemistry

Claisen-Schmidt reaction of commercially available inexpensive acetophenone derivatives (**1a-1d**) and aromatic aldehydes (**2a-2d**) in presence of catalytic amount of sodium hydroxide (10%) in ethanol obtained corresponding chalcones (**3a-3e**) in quantitative yields (>95%) (Scheme 1) [68]. Structures of the compounds **3a-3e** were resolved by systematic analysis of nuclear magnetic resonance (NMR) and mass spectroscopic (MS) data and were compared with the reported values.

Scheme 1. Synthesis of Chalcones (**3a-e**)

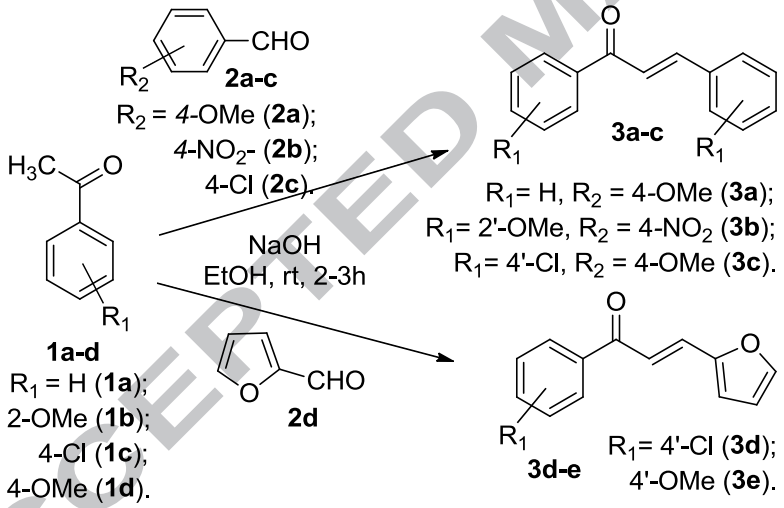

Scheme 1. Synthesis of chalcones (**3a-e**)

On the other hand, 5-nitrofuran-2-carbohydrazide (**4b**) was synthesized using ethyl 5-nitrofuran-2-carboxylate (**4e**) with hydrazine hydrate in absolute ethanol at 0°C for 1h, and benzo[*d*]thiazole-2-carbohydrazide (**4c**) was synthesized using ethyl benzo[*d*]thiazole-2-carboxylate (**4f**) with hydrazine hydrate in refluxing ethanol for

overnight (Scheme 2). Furan-2-carbohydrazide (**4a**) and isonicotinohydrazide (**4d**) were obtained from commercial source.

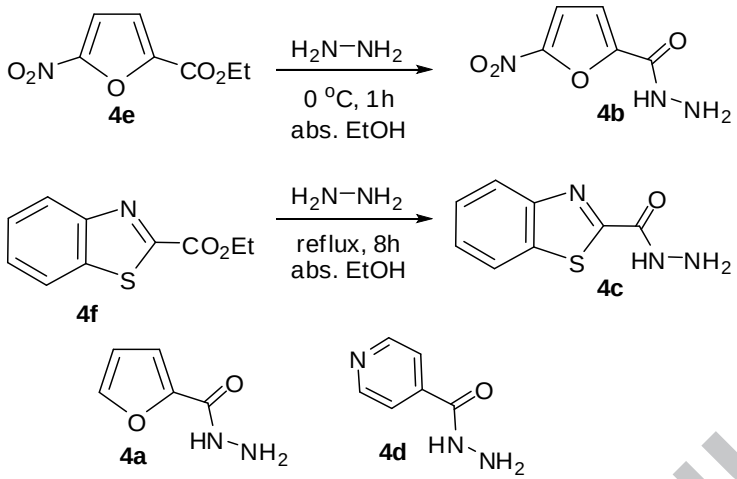

Scheme 2. Synthesized and commercial hydrazides (**4a**-**4d**)

Synthesis of pyrazoline derivatives **5a**-**5i** was straightforward as shown in Scheme 3. Intermediate chalcones (**3a**-**3e**) and hydrazide (**4a**-**4d)** were reacted to obtain pyrazoline derivatives **5a**-**5i** in presence of catalytic amount of glacial acidic acid in ethanol [69]. Purification of the compounds were accomplished by flash column chromatography on silica gel eluting with ethyl acetate and *n*-hexane (1:1) obtained analytical pure **5a**-**5i** (92-96 % yields).

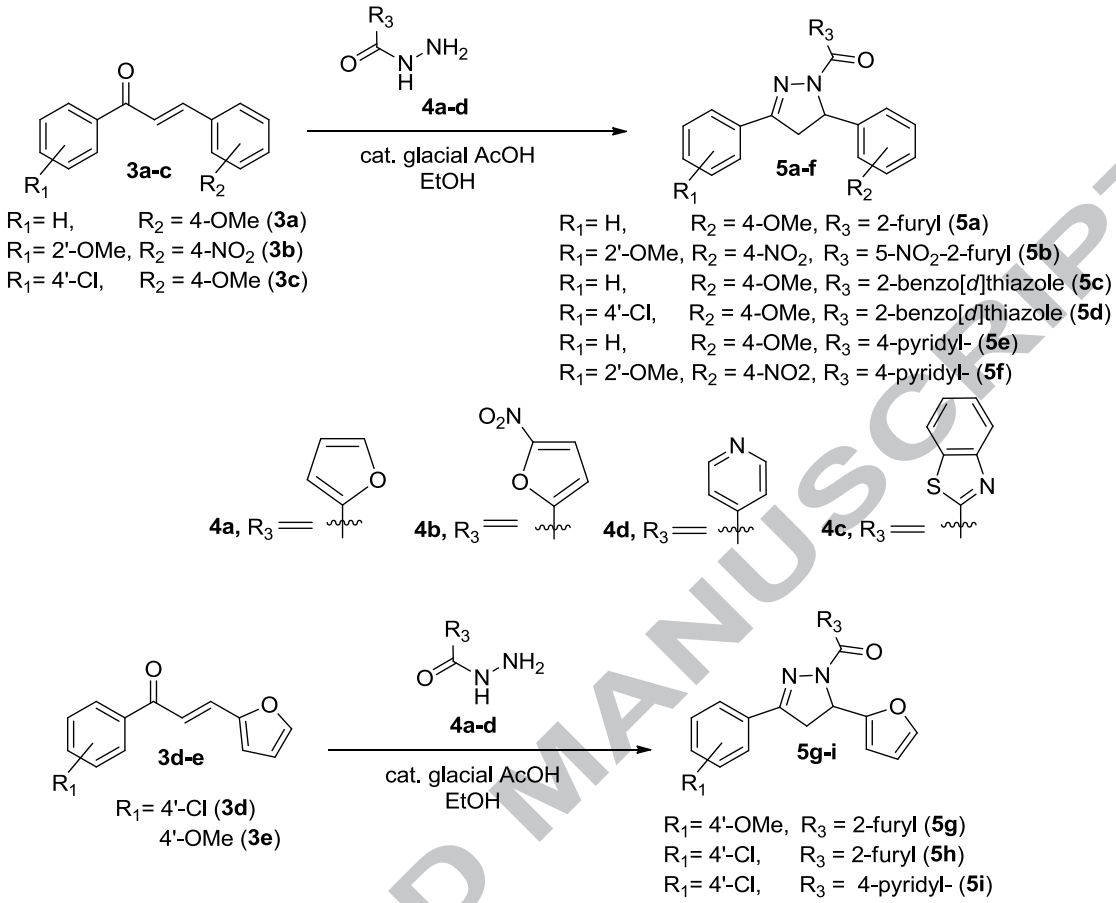

Scheme 3. Synthesis of pyrazoline derivatives (**5a-5i**)

The structures of the compounds were characterized using spectroscopic data as follows: The IR spectra on KBr gives absorption bands in the regions 1612-1510 cm^{-1} corresponding to C=N stretching and 1704-1626 cm^{-1} corresponding to amide carbonyl (N-C=O) stretching. Characteristic methylene protons (4-H_α and 4-H_β) for the compounds (**5a-5f**) were shown at 3.52-4.04 ppm for 4-H_α and at 3.13-3.50 ppm for 4-H_β as double doublet with the coupling constant '*J*' approximately 18.0 & 11.5 Hz for 4-H_α and 18.0 & 4.5 Hz for 4-H_β, respectively. Another characteristic vicinal methine proton 5-H was appeared at 5.68-5.92 ppm as double doublet with the coupling constant 11.5 and 4.5 Hz. Synthesized pyrazoline derivatives also characterized by mass spectrometer, all the derivatives gave protonated $[M+H]^+$

and/or sodium adduct $[M+Na]^+$ of molecular mass in positive mode or deprotonated $[M-H]^-$ molecular mass in negative mode. In addition, the structures of the pyrazoline derivatives also confirmed by elemental analysis data found for carbon, hydrogen and nitrogen (CHN) percentage (details are given in experimental section).

*Recombinant topoisomerase I and II inhibitory activities of compounds **5a-5i**.*

The conversion of supercoiled plasmid DNA to relaxed DNA by recombinant topo I and II was examined in the presence of each **5a-5i** for measuring their topo I and II inhibitory activities. Well-known topo I and II inhibitors, camptothecin and Etoposide were used as positive controls. The reaction products of topo I and II relaxation assays were analysed by electrophoretic mobility and developed in ethidium bromide in the presence of UV light. The inhibitory activities were evaluated at 100 μM for all compounds. Only those compounds with moderate to significant activity were tested further at 20 μM concentration.

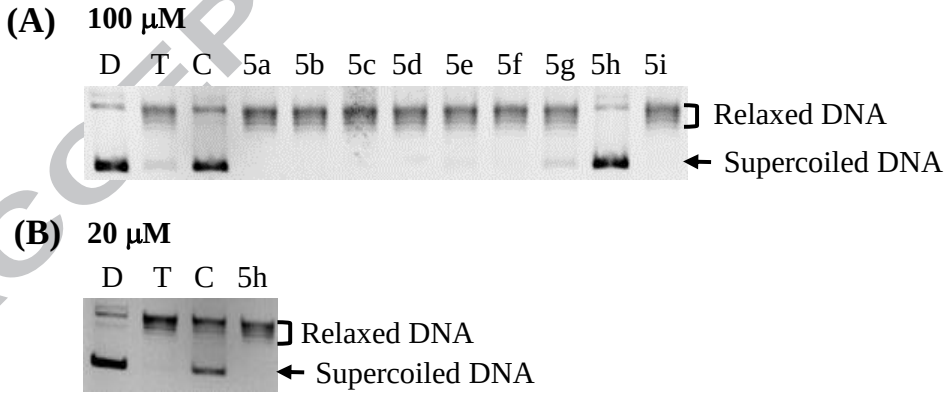

Figure 1. Recombinant topo I inhibitory activities of compounds **5a-5i** at 100 μM (**A**) and 20 μM (**B**). Lane **D**: pBR322 DNA only; Lane **T**: pBR322 DNA + Topo I; Lane **C**: pBR322 DNA + Topo I + Camptothecin; Lanes **5a-5i**: pBR322 DNA + Topo I + compounds **5a-5i**.

As shown in Figure 1, most of the compounds did not exhibit topo I inhibitory activity at 100 μM concentration while compound **5h** showed very strong topo I inhibitory activity of 97% (as compared to 74% of camptothecin) at 100 μM concentration and weak topo I inhibitory activity of 4% (as compared to 25% of camptothecin) at 20 μM concentration.

In case of topo II inhibitory evaluation, we found all the compounds **5a-5i** showed significant topo II inhibitory activity in the range of 90 - 94% (as compared to 96 % of Etoposide) at 100 μM concentration but inactive or very weak at 20 μM concentration (only compounds **5b** and **5h** inhibited topo II by 3% and 1% as compared to 41% of Etoposide).

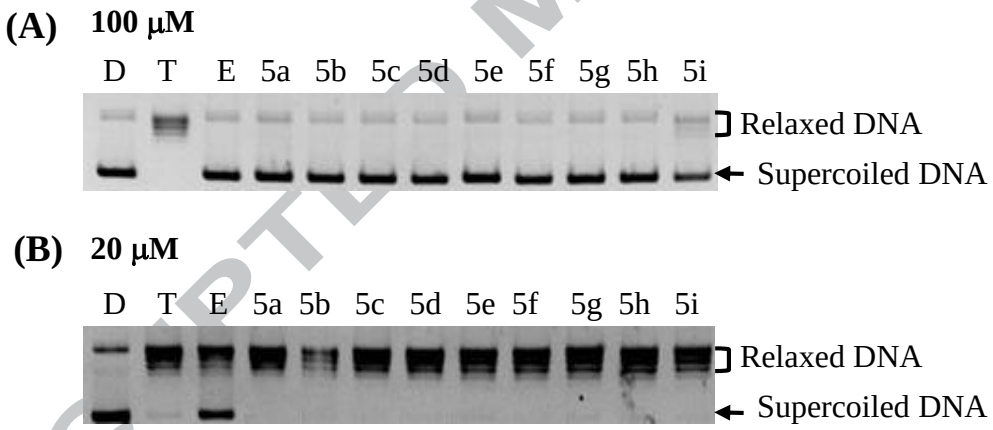

Figure 2. Recombinant topo II inhibitory activities of compounds **5a-5i** at 100 μM (**A**) and 20 μM (**B**). Lane **D**: pBR322 DNA only; Lane **T**: pBR322 DNA + Topo II; Lane **E**: pBR322 DNA + Topo IIα + Etoposide; Lanes **5a-5i**: pBR322 DNA + Topo II + compounds **5a-5i**.

Topo I and topo II inhibitory activities of compounds **5a-5i** at both 100 and 20 μM concentrations are summarized in Table 1. It should be noted that, compound **5h** showed considerable dual topo I and II inhibitory activities.

Table 1. Recombinant topo I and II inhibitory activities of compounds **5a-5i**

Compounds	Topo I (% inhibition)		Topo II (% inhibition)	
Concentration	100 μM	20 μM	100 μM	20 μM
Camptothecin	73.6	24.6	-	-
Etoposide	-	-	95.9	41.1
5a	0.0	-	91.6	0.0
5b	0.0	-	92.6	2.9
5c	0.0	-	91.2	0.0
5d	0.0	-	89.7	0.0
5e	0.0	-	92.5	0.0
5f	0.0	-	92.8	0.0
5g	0.0	-	94.1	0.0
5h	96.8	4.0	93.1	1.3
5i	0.0	-	76.0	0.0

*Antiproliferative activity assays of compounds **5a-5i**.*

For the evaluation of antiproliferative activity of the compounds **5a-5i**, three different human cancer cell lines, HCT15 (human colorectal adenocarcinoma cell line), BT474 (human ductal carcinoma cell line) and T47D (Human ductal breast epithelial tumor cell line) were used. Antiproliferative activity evaluation was performed for **5a-5i** since all had significant topo II inhibitory activity. Antiproliferative activity

evaluation results against human cancer cell lines are listed in Table 2 as values of IC_{50}. Most of the compounds showed strong antiproliferative activity against HCT15 cells with the IC_{50} values of 1.9-10.4 μM, whereas, controls gave IC_{50} values of 23.0, 6.9 and 7.1 μM for Adriamycin, Etoposide and Camptothecin, respectively. Among the compounds, **5b** and **5h** did not show antiproliferative activity (IC_{50} > 50). On the other hand, strong antiproliferative activity against BT474 cells with IC_{50} values of 6.3-7.2 μM was observed for compounds **5c**, **5d**, **5f** and **5i**, whereas controls gave IC_{50} values of 3.2, 6.6 and 7.0 μM for adriamycin, Etoposide and Camptothecin, respectively. Moderate to strong antiproliferative activity was observed for the compounds **5a**, **5d**, **5g** and **5i** against human ductal breast epithelial tumor cell line (T47D).

Table 2. Antiproliferative activity assays of compounds **5a-5i**

Compound	IC_{50} (μM)		
	HCT15	BT474	T47D
Adriamycin	23.0 ± 7.6	3.2 ± 0.1	2.9 ± 0.1
Etoposide	6.9 ± 1.1	6.6 ± 0.1	6.4 ± 0.3
Camptothecin	7.1 ± 2.3	7.0 ± 1.2	4.1 ± 0.1
5a	3.9 ± 0.3	> 50	27.3 ± 2.2
5b	> 50	> 50	> 50
5c	1.9 ± 0.8	6.3 ± 0.1	> 50
5d	4.1 ± 0.01	7.2 ± 0.03	6.6 ± 0.8
5e	10.4 ± 1.1	> 50	> 50
5f	2.6 ± 1.2	7.2 ± 1.1	> 50
5g	4.3 ± 0.1	> 50	7.5 ± 1.1
5h	> 50	> 50	> 50
5i	3.1 ± 0.2	6.5 ± 0.1	7.9 ± 0.8

Structure Activity Relationships (SARs) Study.

The structural activity relationships (SARs) was analyzed based on the antiproliferative activity results of compounds **5a-5i** against HCT15, BT474 and T47D cells lead to the following assumptions. As depicted in Table 3, compound **5a** showed 3.9 μM of IC_{50} against HCT15 cells while Adriamycin, Etoposide and Camptothecin showed 23.0, 6.9 and 7.1 μM, respectively. On the other hand, compound **5a** showed weak or very weak antiproliferative activity against T47D cells (IC_{50} = 27 μM) and BT474 cells (IC_{50} > 50 μM). Introducing substituents in phenyl ring-A with 2'-OCH_3, 4-NO_2 group instead of 4-OCH_3 in phenyl ring-B and 5-NO_2 in

furan ring in compound **5b** almost did not show antiproliferative activity at 50 μM treatment with all tested cells (IC_{50} > 50 μM). While replacing furan ring of compound **5a** by benzo[*d*]thiazole ring to be compound **5c**, antiproliferative activity increased greatly with IC_{50} values of 1.9 μM against HCT15 cells and 6.3 μM against BT474 cells, where IC_{50} values of adriamycin, Etoposide and camptothecin were 3.2, 6.6 and 7.0 μM, respectively. Keeping benzo[*d*]thiazole ring as **5c** and introducing substituent on ring-A with 4'-Cl in compound **5d** improved antiproliferative activity (IC_{50} = 4.1 μM against HCT15, 7.2 μM against BT474 and 6.6 μM against T47D cells) compared to compound **5a**. However, replacing furan ring of compound **5a** or benzo[*d*]thiazole ring of compound **5c** by 4-pyridyl ring to be compound **5e** showed less antiproliferative activity (IC_{50} = 10 μM) against HCT15 cells, and almost no antiproliferative activity with other two cell lines. Interestingly, replacing furan ring of compound **5b** with 4-pyridyl ring to be compound **5f** showed much stronger antiproliferative activity (IC_{50} = 2.6 μM) than all control compounds against HCT15 cells and similar antiproliferative activity (IC_{50} = 7.2 μM) to Etoposide and camptothecin and weaker than Adriamycin against BT474 cells. The subtle modification on the skeleton of compounds **5g-5i** also showed dramatic change in antiproliferative activity. Introducing methoxy group (-OCH_3) in 4'-position of phenyl ring-B of compound **5a** and replacing ring-B by ring-C to be compound **5g** ameliorated antiproliferative activity (IC_{50} = 4.3 μM) against HCT15 cells and showed moderate antiproliferative activity (IC_{50} = 7.5 μM) against T47D cells. Unfortunately, replacement of 4'-OCH_3 of ring-A of **5g** with 4'-Cl to be compound **5h** deteriorated antiproliferative activity (IC_{50} > 50μM). Interestingly, replacing furan ring of compound **5h** by 4-pyridyl ring to be compound **5i** showed excellent antiproliferative

activity (IC_{50} = 3.1 µM) against HCT15 cells and moderate antiproliferative activity (IC_{50} = 6.5 µM and 7.9 µM) against BT474 and T47D cells, respectively.

Table 3. Summarized SARs study results of pyrazoline derivatives **5a-5i**

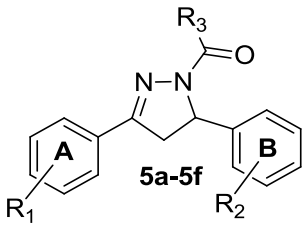

Entry	R	Antiproliferative activity (IC_{50} in μM)
5a	R_1=H; R_2=4-OCH_3; R_3= 	3.9 ± 0.3 against HCT15 cells
5b	R_1=2'-OCH_3; R_2=4-NO_2; R_3= 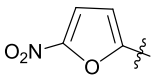	Not active
5c	R_1=H; R_2=4-OCH_3; R_3= 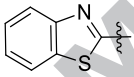	1.9 ± 0.8 against HCT15 cells 6.3 ± 0.1 against BT474 cells
5d	R_1=4'-Cl; R_2=4-OCH_3; R_3= 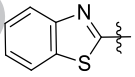	4.1 ± 0.01 against HCT15 cells 7.2 ± 0.03 against BT474 cells 6.6 ± 0.8 against T47D cells
5e	R_1=H; R_2=4-OCH_3; R_3= 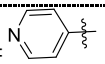	10.3 ± 1.1 against HCT15 cells
5f	R_1=2'-OCH_3; R_2=4-NO_2; R_3= 	2.2 ± 1.2 against HCT15 cells 7.2 ± 1.1 against BT474 cells
	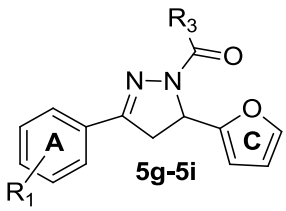	
5g	R_1=4'-OCH_3; R_3= 	4.3 ± 0.1 against HCT15 cells 7.5 ± 1.1 against T47D cells
5h	R_1=4'-Cl; R_3= 	Not active
5i	R_1=4'-Cl; R_3= 	3.1 ± 0.2 against HCT15 cells 6.5 ± 0.1 against BT474 cells

	7.9 ± 0.8 against T47D cells

All the compounds **5a-5i** showed moderate to significant antiproliferative activity even much more potential than control drugs in some cases. Interestingly, most of the compounds **5a-i** did not show topo I inhibitory activity at all, except for compound **5h,** which has 4'-Cl substituent attached with 4'-position of ring-A in the skeleton of compounds **5g-5i**. It inhibited topo I by 97% at 100 μM concentration and 4% at 20 μM concentration, whereas camptothecin inhibited 74%, and 24% at 100 μM and 20 μM, respectively. On the other hand, all compounds **5a-5i** inhibited topo II activity. Substituents did not affect very much to increase or decrease the topo II inhibitory activity. The topo II inhibitory activity of compounds **5a-5i** was comparable with that of Etoposide at 100 μM concentration.

*Molecular docking study of compounds **5a-5i**.*

As discussed above, compounds **5a-5i** inhibited topo II specifically than topo I except for compound **5h**. Topoisomerases resolve DNA topological problems encountered during DNA replication, transcription, recombination, repair and chromatin assembly through breaking and relegating single strand for topo I and double strand of DNA for topo II, respectively [70]. Beside the difference of breaking single or double strands of DNA, topo II is different from topo I in that an ATP binds to the ATPase domain [71]. Therefore, we first checked whether compounds **5a-5i** can bind to the ATPase domain with molecular docking study using coordinates (PDB entry 1ZXM) previously reported for the co-crystal structure of the adenosine 5′-(β,γ-imido) triphosphate tetralithium salt hydrate (AMP-PNP) bound to the ATP-binding domain of human topo II [61, 72]. AMP-PNP is a structural analogue of ATP that has comparable binding affinity for the ATP-binding pocket of topo II but is non-

hydrolyzable which enables to co-crystallize with topo II. AMP-PNP was used as a reference ligand to identify the active site and to validate our docking process by re-docking. Compounds **5a-5i** showed favourable binding to the ATP-binding domain in order of **5b**>**5f**>**5d**. All compounds have a chiral center on the pyrazoline ring. The R and S isomers of all compounds were prepared and molecular docking study were done for all the isomers. Compound **5f** bind to the ATP binding pocket better than compound **5d**. However, the docking result of the two stereoisomers of compound **5f** did not align well (Figure 3A). On the other hand, the two stereoisomers of **5d** flipped over in order to occupy the same binding site (Figure 3). As shown in detailed view of compound **5d** bound to the ATP-binding domain of human topo II (Figure 3), compound **5d** fits well into the ATP-binding cleft drawn in space-filled mode (Figure 3A) and overlays with AMP-PNP (Figure 3B). Compound **5d** has hydrogen-bonds with residues of Arg162 and Gly164 and hydrophobic interactions with Asn91, Asn95, Asn120, Ile141, Phe142, Thr147, Ser148, Ser149, Arg162, Asn163, Gly164, Tyr165, Gly166, Ala167, Gln376, and Lys378 of the topo II ATP-binding pocket. In consideration of the preference from the results of the docking study and antiproliferative activity, compound **5d** was chosen as a representative compound to determine whether it competes with ATP and inhibits ATP hydrolysis, leading to inhibition of topo II catalytic activity.

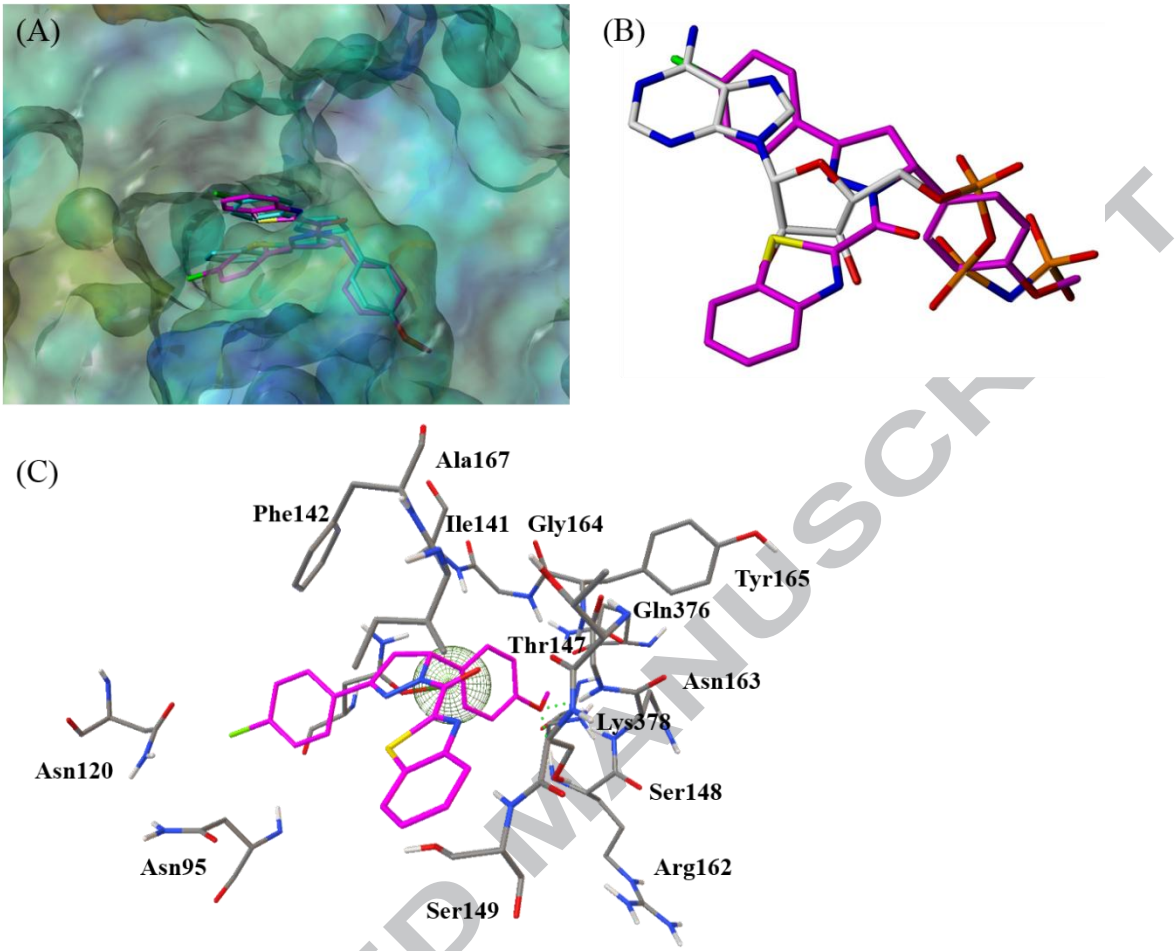

Figure 3. Compound **5d** potentially binds to the ATP binding pocket in the ATPase domain of human topo IIα. (**A**) Magnified view of compound **5d** (**R-5d**, magenta; **S-5d**, cyan) binding to the active site of ATPase domain of topo IIα. The transparent channel surface of the ATP binding pocket is represented and coloured by electrostatic potential (red, most positive; purple, most negative). (**B**) Overlay view of compound **5d** and AMP-PNP (compound **5d**, magenta; AMP-PNP, gray). (**C**) Magnified view of the topo IIα ATP binding pocket. The residues of the topo IIα ATP-binding domain that have van der Waals contact with compound **R-5d** are shown as sticks. The stick representation of the complex is colored by the atom type (**R-5d**, magenta).

*Compound **5d** is ATP-competitive human topo II catalytic inhibitor.*

To confirm compound **5d** binds to the ATP binding pocket of human topo II, we performed ATPase assay which evaluates the degree of ATP hydrolysis of topo II. Compound **5d** inhibited the ATP hydrolysis of topo II at a dose-dependent manner with similar extent to Etoposide, a well-known competitive topo II catalytic inhibitor (Figure 4A) [73]. The ATP competition assay with topo II was performed as the same procedure as the topo II relaxation assay, using different concentration of ATP of 1 and 2 mM. Compound **5d** inhibited the topo II activity in ATP concentration-dependent manner (Figure 4B and 4C), while Etoposide did not change the activity as the ATP concentration increased which is depicted by bar graphs in Figure 4C. It reflected compound **5d** functioned as an ATP-competitive manner but Etoposide did not. We further performed the cleavage complex assay to investigate compound **5d** as a topo II catalytic inhibitor. Topo II poisons act by stabilizing transiently-formed topo II enzyme-DNA cleavage complex leading to the formation of linear DNA [74]. In cleavage complex assay, initially the relaxation of the pBR322 plasmid was allowed by the addition of topo IIα and then compound **5d** was treated. In contrast to Etoposide, a well-known topo II poison, linear form of DNA did not form in the case of compound **5d** up to 300 μM treatment, which inferred no stabilization of enzyme-DNA cleavage complex, (Figure 4D). Taken together, compound **5d** acted as an ATP-competitive catalytic inhibitor rather than a topo II poison.

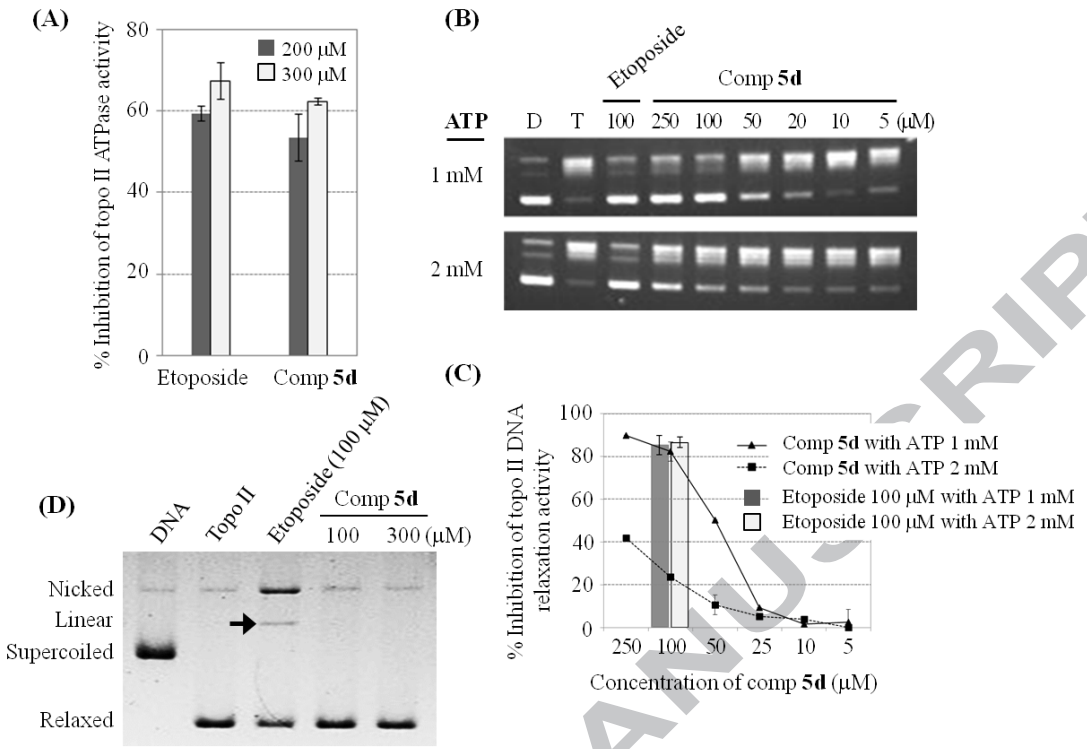

Figure 4. The evaluation of compound **5d** functioning as an ATP-competitive topo II catalytic inhibitor. (**A**) ATPase assay. Topo II-mediated ATPase assay was performed with ATP dehydrogenase reaction. The free phosphate derived by hydrolysis reaction of recombinant human topo IIα was detected by malachite green phosphate assay reagent with incubation for 30 min at room temperature. The extent of hydrolysis reaction was determined by measuring absorbance of green complex formed between malachite green, molybdate and free phosphate at a wavelength of 620 nm using ELISA micro-plate reader. (B) ATP competition assay. Except for the concentration of ATP, ATP competition assay was performed as following the same process as the DNA topo II-mediated DNA relaxation assay. The final concentrations of ATP were 1 mM and 2 mM. Etoposide was used as a positive control. (C) The quantitative results in (B) were depicted. (D) Cleavage complex assay. 100 ng/μL of supercoiled DNA pBR322 was incubated with 3 unit of recombinant human DNA topo IIα for 5 min followed by the addition of compound **5d**. The linear form of DNA was arrow-labelled after reaction mixture was electrophoresed in 1% agarose gel in TAE buffer

containing 0.5 µg /mL ethidium bromide followed by visualized gel using an Alpha Tech Imager.

*Compound **5d** inhibited endogenous topos with better potency than Etoposide.*

To confirm the effect of compound **5d** on endogenous topo-mediated DNA relaxation in cells, we prepared nuclear lysates of HCT15 cells treated with compound **5d** and Etoposide, respectively, for 24 hr. Untreated nuclear extract was used as a negative control to confirm whether endogenous topo relaxes supercoiled pBR322 plasmid by incubating for 30 min at 37 °C as shown in the second lane of Figure 5. Compound **5d** inhibited the endogenous topo-mediated pBR322 plasmid relaxation more efficiently than Etoposide; % inhibition of DNA relaxation of compound **5d** is 78.0 ± 4.7% at 50 µM; that of Etoposide is 36.0 ± 1.7% at the same concentration (Figure 5).

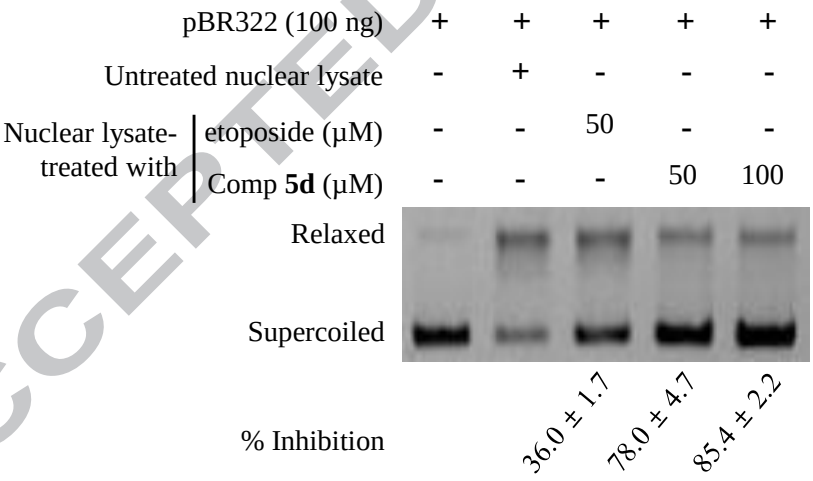

Figure 5. The effect of compound **5d** on endogenous topo-mediated DNA relaxation. Nuclear lysates of HCT15 cells, prepared after treatment with Etoposide and compound **5d** for 24 hr, were incubated for 30 min with 100 ng of pBR322 plasmid at 37 °C.

Conclusion

We have designed and synthesized a series of novel pyrazoline derivatives (**5a-5i**) in two steps via chalcones (**3a-3e**) and 2-carbohydrazide (**4a-4d**). These compounds were evaluated for their antiproliferative activity and topo I and II inhibitory activities. Among them **5a**, **5c-d**, **5f-g** and **5i** displayed excellent antiproliferative activity against HCT15 cell lines; **5c**, **5d**, **5f** and **5i** against BT474 cell lines; and **5d**, **5g** and **5i** against T47D cell lines. All the pyrazoline derivatives (**5a-5i**) inhibited topo II activity with specificity over topo I, except compound **5h** (96.8% at 100 μM and 4.0% at 20 μM concentration). We further determined the mode of action of a representative compound **5d** as an ATP-competitive topo II catalytic inhibitor. Compound **5d** inhibited topo II catalytic activity through binding to the ATPase domain of topo II in ATP-competitive manner without generating the linear DNA which was confirmed by docking study, ATP competition, ATPase, and cleavage complex assays using recombinant human topo IIα. Compound **5d** inhibited endogenous topo (78.0% at 50 μM) with better potency than Etoposide (36.0% at 50 μM). Modification of the structures of the compound and the animal study are in progress for further development of novel anticancer agents and the results will be explored in due courses.

Experimental

General Chemistry

Chemicals and solvents were reagent grades and were used without further purifications. Compounds **4a**, **4d**, **4e** and **4f** were obtained from commercial sources. Thin layer column chromatography (TLC) analysis was carried out on glass-backed TLC silica plates (silica gel 60 F_{254}, 0.25 mm) impregnated with fluorescence indicator

(Merck art. 1.05554). Column chromatography was carried out on 60-120 mesh Merck silica gel. Melting points were determined on a Fisher Scientific^{TM} digital melting point apparatus (model number IA9100) and are uncorrected. Infrared spectra (IR) were recorded using KBr pellets for solids and neat for liquids on a PerkinElmer Spectrum BX FTIR spectrometer. NMR spectra were obtained using 500 MHz Avance Bruker Ultra Shield^{TM} and an Agilent technologies premium shielded 400 MHz spectrometer and are reported as parts per million (ppm) from the internal standard of tetramethylsilane. Chemical shift for ^{1}H- and ^{13}C-NMR (δ) are reported in ppm. The working frequency for ^{1}H- and ^{13}C- were 500/400 MHz and 125/100 MHz, respectively. $CDCl_3$, and DMSO-*d6* were used as internal standard in ^{1}H- as 7.24 and 2.49 ppm, while in ^{13}C- as 77 and 39.5 ppm, respectively. The coupling constants *J* are reported in Hertz (Hz). Peaks were described as broad singnals (br), singlet (s), doublets (d), doublets of doublets (dd), doublets of doublets of doublets (ddd), triplets (t) and multiplets (m), doublets of triplets (dt), triplets of doublets (td). Mass spectra were carried out using an Agilent High performance liquid chromatography (HPLC) 1200 connected with Agilent 6320 Ion Trap mass spectrometer fitted with ESI ion source in positive and/or negative mode. Elemental Analysis were perform using a PerkinElmer 2400 CHN analyzer.

General procedure for the preparation of Chalcone (3a-3e).

An equimolar mixture of (substituted)-acetophenone and (substituted)-benzaldehyde in ethanol in presence of alcoholic sodium hydroxide (10%) was stirred for 2-3 hours. The whole mass of the mixture was poured into ice cold water, solid precipitate was filtered, dried in open air, obtained quantitative yields of the corresponding chalcones (**3a-3d**). Crystallization from ethanol afforded the pure chalcones, and the spectral

data were identical to those of literature values and for unreported compounds are given below.

(E)-3-(4-methoxyphenyl)-1-phenylprop-2-en-1-one (3a). White solid; (CAS no. 959-33-1); (98 %); mp. = 61°C [lit. [75] mp. = 60-63°C]; ^{1}HNMR ($CDCl_3$, 400 MHz): δ 8.01 (dt, *J* = 6.8, 1.2 Hz, 2H), 7.79 (d, *J* = 15.6 Hz, 1H), 7.60 (dt, *J* = 8.4, 1.6 Hz, 2H), 7.56 (dt, *J* = 8.8 Hz, 1H), 7.50 (d, *J* = 7.6 Hz, 1H), 7.49 (t, *J* = 8.8 Hz, 1H), 7.42 (d, *J* = 15.6 Hz, 1H), 6.97 (dt, *J* = 8.8, 2.0 Hz, 1H), 3.85 (s, 3H, -OCH3); ^{13}CNMR ($CDCl_3$, 100 MHz): δ 190.59, 161.69, 144.70, 138.52, 132.54, 130.23, 128.56, 128.41, 127.63, 119.80, 114.42 and 55.40 ppm. ESI mass (*m/z*) 238.9 $[M+H]^+$, 260.9 $[M+Na]^+$ (calculated exact mass 238.1).

(E)-1-(2-methoxyphenyl)-3-(4-nitrophenyl)prop-2-en-1-one (3b). Yellow solid; (96 %); mp. = 71-72°C; ^{1}H NMR ($CDCl_3$, 500 MHz): δ 8.17 (d, *J* = 8.5 Hz 2H), 7.65 (d, *J* = 8.5 Hz 2H), 7.61-7.56 (overlapped, 2H), 7.48-7.42 (overlapped, 2H), 6.98 (d, *J* = 7.5 Hz, 1H), 6.95 (d, *J* = 9.0 Hz, 1H), 3.86 (s, 3H, -OCH_3) ppm; ^{13}C NMR ($CDCl_3$, 125 MHz): δ 190.64, 157.45, 147.31, 140.52, 138.18, 132.71, 129.70, 129.63, 127.80, 127.52, 123.11, 119.95, 110.70 and 54.79 ppm. ESI mass (*m/z*) 284.0 $[M+H]^+$, 305.9 $[M+Na]^+$ (calculated exact mass 283.1).

(E)-1-(4-chlorophenyl)-3-(4-methoxyphenyl)prop-2-en-1-one (3c). White solid; (98 %); mp. = 117-118°C [lit. [76] mp. = 117°C]; ^{1}HNMR ($CDCl_3$, 400 MHz): δ 7.95 (dt, *J* = 8.8, 2.0 Hz, 2H), 7.79 (d, *J* = 15.6 Hz, 1H), 7.60 (dt, *J* = 8.8, 1.6 Hz, 2H), 7.46 (dt, *J* = 8.8, 2.0 Hz, 2H), 7.36 (d, *J* = 16.0 Hz, 1H), 6.94 (dt, *J* = 8.8, 2.0 Hz, 2H), 3.85 (s, 3H, -OCH3); ^{13}CNMR ($CDCl_3$, 100 MHz): δ 189.18, 161.85, 145.20, 138.93, 136.81,

130.32, 129.82, 128.85, 127.43, 119.17, 114.70 and 55.42 ppm. ESI mass (*m/z*) 273.1 $[M+H]^+$, 294.9 $[M+Na]^+$ (calculated exact mass 272.1).

(E)-1-(4-chlorophenyl)-3-(furan-2-yl)prop-2-en-1-one (3d). CAS no. 114570-70-6; White solid; lit. [77] (95 %); ^{1}HNMR ($CDCl_3$, 400 MHz): δ 7.95 (dt, *J* = 8.8, 2.4 Hz, 2H), 7.58 (d, *J* = 15.2 Hz, 1H), 7.51 (d, *J* = 1.2 Hz, 1H), 7.44 (dt, *J* = 8.8, 2.0 Hz, 2H), 7.38 (d, *J* = 15.2 Hz, 1H), 6.72 (d, *J* = 2.8 Hz, 1H), 6.50 (dd, *J* = 3.6, 2.0 Hz, 1H); ^{13}CNMR ($CDCl_3$, 100 MHz): δ 188.39, 151.52, 145.10, 139.15, 136.44, 131.03, 129.81, 128.89, 118.66, 116.63 and 112.76 ppm. ESI mass (*m/z*) 232.9 $[M+H]^+$, 254.8 $[M+Na]^+$ (calculated exact mass 233.0).

(E)-1-(4-methoxyphenyl)-3-(furan-2-yl)prop-2-en-1-one (3e). White solid; (98 %); mp. = 68-69°C [lit. [78] mp. = 68°C]; ^{1}HNMR ($CDCl_3$, 400 MHz): δ 8.04 (dt, *J* = 9.2, 2.0 Hz, 2H), 7.57 (d, *J* = 15.6 Hz, 1H), 7.51 (dd, *J* = 2.4, 1.2 Hz, 1H), 7.45 (d, *J* = 15.2 Hz, 1H), 6.96 (dt, *J* = 8.8, 2.0 Hz, 2H), 6.68 (d, *J* = 3.6 Hz, 1H), 6.49 (dd, *J* = 3.6, 2.0 Hz, 1H), 3.87 (s, 3H, -OCH3); ^{13}CNMR ($CDCl_3$, 100 MHz): δ 188.05, 163, 40, 151.82, 144.67, 131.08, 130.72, 129.96, 119.21, 115.75, 113.82, 112.58 and 55.47 ppm. ESI mass (*m/z*) 228.9 $[M+H]^+$, 250.8 $[M+Na]^+$ (calculated exact mass 228.0);

General procedure for the preparation of Hydrazide (4a-4d).

Furan-2-carbohydrazide (4a). (CAS no. 3326-71-4) are commercial available; mp. = 77-79°C. ^{1}H NMR ($CDCl_3$, 500 MHz): δ 7.45 (d, *J* = 1.0 Hz 1H), 7.15 (d, *J* = 2.5 Hz 1H), 7.50 (dd, *J* = 3.5, 1.0 Hz, 1H). . ^{13}C NMR ($CDCl_3$, 125 MHz): δ159.47, 146.64, 144.32, 114.76 and 111.99 ppm. ESI mass (*m/z*) 126.9 $[M+H]^+$ (calculated for 129.1).

5-Nitrofuran-2-carbohydrazide (4b). A solution of hydrazine hydrate (11 mmol) and ethyl 5-nitrofuran-2-carbohydrazide (10 mmol) in absolute ethanol (100 ml.) was stirred at 0 °C for 1 h. the stirring was continued for further 1h at room temperature. The solid formed was filtered off and washed with ethanol and dried by suction. Crystallization from methanol afforded 5-nitrofuran-2-carbohydrazide (**4b**) as pale yellow needles in 73% yield, mp. = 171-172°C [lit. [79] mp. = 171-172°C]; ^{1}HNMR ($CDCl_3$ + DMSO-d_6, 400 MHz): δ 7.22 (d, *J* = 4.0 Hz, 1H), 7.18 (d, *J* = 4.0 Hz, 1H); ^{13}CNMR ($CDCl_3$ + DMSO-d_6, 100 MHz): δ 156.45, 147.22, 115.82 and 112.19 ppm. ESI mass (*m/z*) 171.8 $[M+H]^+$ (calculated exact mass 171.0); CAS no. 5469-78-3.

Benzo[d]thiazole-2-carbohydrazide (4c). A solution of hydrazine hydrate (22 mmol) and ethyl benzo[*d*]thiazole-2-carboxylate (10 mmol) in absolute ethanol (50 mL) was refluxed for 1 h. The solid formed was filtered off and washed with ethanol, dried and crystallization from ethanol afforded benzo[d]thiazole-2-carbohydrazide (**4c**) as pale yellow crystals in 90% yield, mp. = 175-176 °C [lit. [80] mp. 175-176°C]; ^{1}HNMR ($CDCl_3$ + DMSO-d_6, 400 MHz): δ 7.99 (ddd, *J* = 8.0, 1.6, 0.4 Hz, 1H), 7.95 (ddd, *J* = 8.0, 1.6, 0.4 Hz, 1H), 7.48 (td, *J* = 7.2, 1.6 Hz, 1H); 7.43 (td, *J* = 7.2, 1.6 Hz, 1H); ^{13}CNMR ($CDCl_3$ + DMSO-d_6, 100 MHz): δ 163.07, 159.09, 153.11, 136.28, 126.91, 126.76, 124.22 and 122.51 ppm. ESI mass (*m/z*) 193.8 $[M+H]^+$ (calculated exact mass 193.0); CAS number: 28891-34-1.

Isonicotinohydrazide (4d). (CAS no. 54-85-3) are commercial available. ^{1}HNMR ($CDCl_3$ + DMSO-d_6, 400 MHz): δ 8.59 (dd, *J* = 4.4, 1.6 Hz, 2H), 7.67 (dd, *J* = 4.8, 1.6 Hz, 2H); ^{13}CNMR ($CDCl_3$ + DMSO-d_6, 100 MHz): δ 164.95, 150.18, 140.31 and 121.30 ppm. ESI mass (*m/z*) 137.9 $[M+H]^+$ (calculated exact mass 137.0).

General procedure for the preparation of Pyrazoline (5a-5i).

A mixture of chalcone (1 equiv.) and hydrazide (1.2 equiv.) was refluxed overnight in ethanol in the presence of catalytic amount of glacial acetic acid (1-3 drop). Excess solvent were evaporated and the reaction mixture were pass through silica gel column chromatography using ethyl acetate and *n*-hexane as solvent. The spectral data for unreported compounds follows.

Furan-2-yl(5-(4-methoxyphenyl)-3-phenyl-4,5-dihydro-1H-pyrazol-1-yl)methanone (5a). Light brown solid; (94 %); mp = 243-244°C; IR (KBr, cm^{-1}): 3116, 3062, 2953, 1648, 1611, 1560, 1512, 1472, 1429, 1246, 1174, 1036 cm^{-1}; ^{1}H NMR ($CDCl_3$, 500 MHz): δ 7.23-7.16 (m, 2H), 7.59 (d, *J* = 2.5 Hz 1H), 7.53 (s, 1H), 7.39-7.37 (m, 3H), 7.14 (d, *J* = 8.5 Hz, 2H), 6.76 (d, *J* = 9.0 Hz, 2H), 6.48 (t, *J* = 1.5 Hz, 1H) 5.68 (dd, *J* = 11.5, 4.0 Hz, 1H), 3.68 (s, 3H, $-OCH_3$), 3.66 (overlapped, 1H), 3.13 (dd, *J* = 18.0, 4.0 Hz, 1H), ppm; ^{13}C NMR ($CDCl_3$, 125 MHz): δ 159.11, 155.86, 155.40, 146.37, 145.37, 133.67, 131.39, 130.56, 128.87, 127.13, 126.81, 118.94, 114.25, 111.52 60.58, 55.30 and 41.26 ppm; ESI mass (*m/z*) 347.1 $[M+H]^+$ (calculated exact mass 346.1); *Anal*. Calculated for $C_{21}H_{18}N_2O_3$: C, 72.82; H, 5.24; N, 8.09. Found: C, 72.03; H, 5.24; N, 7.87.

(3-(2-Methoxyphenyl)-5-(4-nitrophenyl)-4,5-dihydro-1H-pyrazol-1-yl)(5-nitrofuran-2-yl)methanone (5b). Yellow solid; (92 %); mp = 140-141°C; IR (KBr, cm^{-1}): 3326, 3106, 3060, 2949, 1704, 1596, 1513, 1470, 1257, 1031 cm^{-1}; ^{1}H NMR ($CDCl_3$, 500 MHz): δ 7.82 (s, 2H), 7.69 (s, 1H), 7.63 (s, 1H), 7.49 (m, 2H), 7.25 (d, *J* = 8.5 Hz, 2H), 6.86 (d, *J* = 8.5 Hz, 2H), 6.58 (s, 1H), 5.80 (dd, *J* = 11.5, 4.0 Hz, 1H), 3.79 (s, 3H, $-OCH_3$), 3.77 (overlapped, 1H), 3.24 (dd, *J* = 18.0, 4.0 Hz, 1H), ppm; ^{13}C NMR

($CDCl_3$, 125 MHz): δ 159.13, 155.86, 155.36, 146.39, 145.36, 133.68, 131.41, 130.55, 128.86, 127.14, 126.80, 118.91, 114.26, 111.50 60.58, 55.30 and 41.25 ppm; ESI mass (*m/z*) 434.5 $[M-H]^-$ (calculated exact mass 436.0); *Anal*. Calculated for $C_{21}H_{16}N_4O_7$: C, 57.80; H, 3.70; N, 12.84. Found: C, 57.69; H, 3.77; N, 12.95.

Benzo[d]thiazol-2-yl(5-(4-methoxyphenyl)-3-phenyl-4,5-dihydro-1H-pyrazol-1-yl)methanone (5c). Off white solid; (92 %); mp = 199-200°C; IR (KBr, cm^{-1}): 3062, 2957, 1646, 1610, 1513, 1469, 1417, 1249, 1184, 1036 cm^{-1}; ^1H NMR (DMSO-d_6, 500 MHz): δ 8.29 (d, *J* = 7.0 Hz, 1H), 8.21 (d, *J* = 6.0 Hz, 1H), 7.96 (s, 2H), 7.63-7.56 (m, 5H), 7.25 (d, *J* = 8.0 Hz, 2H), 6.93 (d, *J* = 8.5 Hz, 2H), 5.83-5.81 (m, 1H), 4.01 (dd, *J* = 18, 11.5 Hz, 1H), 3.73 (s, 3H, $-OCH_3$), 3.34 (overlapped, 1H) ppm; ^{13}C NMR (DMSO-d_6, 125 MHz): δ 158.69, 157.46, 155.05, 151.41, 136.76, 133.19, 131.06, 130.54, 128.99, 127.35, 127.16, 127.15, 126.88, 124.43, 122.53, 114.14, 60.65, 55.10 and 41.57 ppm; ESI mass (*m/z*) 414.0 $[M+H]^+$, 436.0 $[M+Na]^+$ (calculated exact mass 413.1); *Anal*. Calculated for $C_{24}H_{19}N_3O_2S$: C, 69.71; H, 4.63; N, 10.16. Found: C, 68.81; H, 4.76; N, 10.21.

Benzo[d]thiazol-2-yl(3-(4-chlorophenyl)-5-(4-methoxyphenyl)-4,5-dihydro-1H-pyrazol-1-yl)methanone (5d). White solid; (94%); mp = 139-140°C; IR (KBr, cm^{-1}): 3012, 1918, 1648, 1593, 1515, 1430, 1400, 1333, 1252, 1178, 1031 cm^{-1}; ^1H NMR ($CDCl_3$, 500 MHz): δ 8.74 (m, 2H), 7.80 (m, 2H), 7.62 (d, *J* = 8.5 Hz, 2H), 7.39 (d, *J* = 8.5 Hz, 2H), 7.25 (d, *J* = 8.0 Hz, 2H), 6.88 (d, *J* = 8.5 Hz, 2H), 5.75 (dd, *J* = 11.5, 4.0 Hz, 1H), 3.76 (s, 3H, $-OCH_3$), 3.76 (overlapped, 1H), 3.21 (dd, *J* = 18.0, 4.5 Hz, 1H) ppm; ^{13}C NMR ($CDCl_3$, 125 MHz): δ 171.12, 164.25, 159.32, 154.90, 149.70, 141.74, 136.76, 133.19, 130.00, 129.47, 128.09, 127.09. 123.65, 114.43, 60.92, 55.29

and 41.60 ppm; ESI mass (*m/z*) 448.3 $[M(^{35}Cl)+H]^+$, 450.3 $[M(^{37}Cl)+H]^+$, 470.4 $[M+Na]^+$ (calculated exact mass 447.1); *Anal.* Calculated for $C_{24}H_{18}ClN_3O_2S$: C, 64.35; H, 4.05; N, 9.38. Found: C, 67.19; H, 4.82; N, 10.61.

(5-(4-Methoxyphenyl)-3-phenyl-4,5-dihydro-1H-pyrazol-1-yl)(pyridin-4-yl)methanone (5e). White solid; (93%); mp = 187-188°C; IR (KBr, cm^{-1}): 3028, 2947, 1641, 1593, 1516, 1454, 1439, 1339, 1244, 1182, 1034 cm^{-1}; ^1H NMR ($CDCl_3$, 500 MHz): δ 8.76 (d, *J* = 3.0 Hz, 2H), 7.86 (d, *J* = 3.0 Hz, 2H), 7.73 (d, *J* = 6.5 Hz, 2H), 3.46 (overlapped, 1H), 7.46 (d, *J* = 7.5 Hz, 2H), 7.29 (d, *J* = 8.0 Hz, 2H), 6.90 (d, *J* = 8.5 Hz, 2H), 5.77 (dd, *J* = 16.5 Hz, 1H), 3.83 (overlapped, 1H), 3.80 (s, 3H, -OCH_3), 3.28 (dd, *J* = 18.0, 4.5 Hz, 1H) ppm; ^{13}C NMR ($CDCl_3$, 125 MHz): δ 164.17, 159.29, 156.04, 149.62, 141.90, 133.37, 130.94, 130.83, 128.88, 127.14, 126.87, 123.78, 114.42, 60.80, 55.31 and 41.68 ppm; ESI mass (*m/z*) 458.0 $[M+H]^+$, 480.0 $[M+Na]^+$ (calculated exact mass 457.1)*; Anal.* Calculated for $C_{22}H_{19}N_3O_2$: C, 73.93; H, 5.36; N, 11.76. Found: C, 73.88; H, 5.06; N, 11.65.

(3-(2-Methoxyphenyl)-5-(4-nitrophenyl)-4,5-dihydro-1H-pyrazol-1-yl)(pyridin-4-yl)methanone (5f). White creamy solid; (93 %); mp = 156-157°C; IR (KBr, cm^{-1}): 3041, 2937, 1701, 1625, 1599, 1516, 1490, 1428, 1340, 1245, 1122, 1024 cm^{-1}; ^1H NMR ($CDCl_3$, 500 MHz): δ 8.77 (dd, *J* = 4.5, 1.5 Hz, 2H), 8.24 (d, *J* = 8.5 Hz, 2H), 7.89 (dd, *J* = 4.5, 1.5 Hz, 2H), 7.84 (dd, *J* = 7.5, 1.5 Hz, 1H), 7.53 (d, *J* = 7.5 Hz, 2H), 7.46 (td, *J* = 7.5, 1.5 Hz, 1H), 7.04 (t, *J* = 7.5 Hz, 1H), 6.99 (d, *J* = 8.5 Hz, 1H), 5.82 (dd, *J* = 11.5, 5.0 Hz, 1H), 4.04 (dd, *J* = 18.0, 12.0 Hz, 1H), 3.88 (s, 3H, -OCH_3), 3.42 (dd, *J* = 18.0, 5.0 Hz, 1H) ppm; ^{13}C NMR ($CDCl_3$, 125 MHz): δ 164.18, 158.47, 155.99, 149.68, 148.54, 147.50, 141.28, 132.47, 129.33, 126.86, 124.40, 123.80,

121.08, 119.37, 11.72, 60.79, 55.53 and 44.66 ppm; ESI mass (*m/z*) 403.1 $[M+H]^+$, 425.0 $[M+Na]^+$ (calculated exact mass 402.1); *Anal*. Calculated for $C_{22}H_{18}N_4O_4$: C, 65.64; H, 4.51; N, 13.92. Found: C, 65.04; H, 4.48; N, 13.93.

Furan-2-yl(5-(furan-2-yl)-3-(4-methoxyphenyl)-4,5-dihydro-1H-pyrazol-1-yl)methanone (5g). White solid; (95 %); mp = 159-160°C; IR (KBr, cm^{-1}): 3141, 3120, 3007, 2968, 2836, 1636, 1607, 1558, 1473, 1435, 1331, 1246, 1148, 1040, 1018 cm^{-1}; ^1H NMR ($CDCl_3$, 500 MHz): δ 7.77 (d, *J* = 8.5 Hz, 2H), 7.65 (d, *J* = 12.0 Hz, 2H), 7.30 (d, *J* = 15.5 Hz, 2H), 7.00 (d, *J* = 8.5 Hz, 1H), 6.57 (d, *J* = 1.5 Hz, 1H), 6.44 (s, 1H), 6.34 (s, 1H), 5.92 (dd, *J* = 11.0, 3.5 Hz, 1H), 3.90 (s, 3H, $-OCH_3$), 3.60 (dd, *J* = 17.5, 11.5 Hz, 1H), 3.50 (dd, *J* = 16.5, 3.5 Hz, 1H) ppm; ^{13}C NMR ($CDCl_3$, 125 MHz): δ 161.56, 155.78, 155.35, 151.66, 146.27, 145.34, 141.96, 128.45, 123.86, 118.98, 114.27, 111.51, 110.63, 108.15, 55.45, 54.33 and 37.19 ppm; ESI mass (*m/z*) 337.0 $[M+H]^+$, 359.0 $[M+Na]^+$ (calculated exact mass 336.1); *Anal*. Calculated for $C_{19}H_{16}N_2O_4$: C, 67.85; H, 4.79; N, 8.33. Found: C, 67.62; H, 4.38; N, 8.21.

(3-(4-Chlorophenyl)-5-(furan-2-yl)-4,5-dihydro-1H-pyrazol-1-yl)(furan-2-yl)methanone (5h). Off white solid; (96 %); mp = 186-187°C; IR (KBr, cm^{-1}): 3131, 3110, 2962, 1635, 1597, 1557, 1470, 1439, 1400, 1329, 1226, 1152, 1011 cm^{-1}; ^1H NMR ($CDCl_3$, 500 MHz): δ 7.66 (d, *J* = 8.5 Hz, 2H), 7.54 (d, *J* = 11.5 Hz, 2H), 7.37 (d, *J* = 8.5 Hz, 2H), 7.21 (s, 1H), 6.48 (s, 1H), 6.35 (s, 1H), 6.18 (s, 1H), 5.84 (dd, *J* = 17.5, 11.5 Hz, 1H), 3.52 (dd, *J* = 17.5, 11.5 Hz, 1H), 3.41 (dd, *J* = 17.5, 4.5 Hz, 1H) ppm; ^{13}C NMR ($CDCl_3$, 125 MHz): δ 155.91, 154.41, 151.29, 146.04, 145.57, 142.08, 136.60, 129.77, 129.15, 128.02, 119.13, 111.58, 110.69, 108.31, 54.60 and 36.99. ESI mass (*m/z*) 341.1 $[M+H]^+$, 363.0 $[M+Na]^+$ (calculated exact mass 340.1); *Anal.*

Calculated for $C_{18}H_{13}ClN_2O_3$: C, 63.44; H, 3.85; N, 8.22. Found: C, 62.99; H, 4.39; N, 8.31.

(3-(4-Chlorophenyl)-5-(furan-2-yl)-4,5-dihydro-1H-pyrazol-1-yl)(pyridin-4-yl)methanone (5i). Light brown solid; (96 %); mp = 156-157°C; IR (KBr, cm^{-1}): 3041, 2925, 1626, 1542, 1441, 1335, 1214, 1146, 1092, 1010 cm^{-1}; ^{1}H NMR ($CDCl_3$, 500 MHz): δ 8.76 (s, 2H), 8.04 (s, 2H), 7.55 (d, *J* = 8.0 Hz, 2H), 7.35 (d, *J* = 8.0 Hz, 2H), 7.29 (s, 1H), 6.42 (s, 1H), 6.31 (s, 1H), 5.84 (dd, *J* = 17.5, 10.5 Hz, 1H), 3.60 (dd, *J* = 17.5, 11.5 Hz, 1H), 3.49 (dd, *J* = 17.5, 4.0 Hz, 1H) ppm; ^{13}C NMR ($CDCl_3$, 125 MHz): δ 157.16, 150.95, 145.05, 139.80, 137.37, 132.18, 124.05, 123.54, 122.93, 120.30, 105.56, 103.76, 49.58 and 32.43. ESI mass (*m/z*) 352.0 [M (^{35}Cl)+H]$^+$, 354.0 [M (^{37}Cl)+H]$^+$ (calculated exact mass 351.1); *Anal*. Calculated for $C_{19}H_{14}ClN_3O_2$: C, 64.87; H, 4.01; N, 11.94. Found: C, 64.08; H, 4.17; N, 10.58.

DNA topo I and II mediated relaxation assay in vitro.

DNA topo I inhibition assay was determined following the method reported by Fukuda *et al* [81] with minor modifications. The tested compounds were dissolved in DMSO at a concentration of 20 mM as stock solutions. The activity of DNA topo I was determined by assessing the relaxation of supercoiled DNA pBR322. The mixture of 100 ng of pBR322 DNA (Fermentas, USA) and 1 unit of recombinant human DNA topo I (TopoGEN INC., USA) was incubated with and without the prepared compounds at 37 °C for 30 min in the relaxation buffer (10 mM Tris-HCl pH 7.9), 150 mM NaCl, 0.1% bovine serum albumin, 1 mM spermidine, 5% glycerol). The reaction in the final volume of 10 µL was terminated by adding 2.5 µL of the stop solution containing 5% sarcosyl, 0.0025% bromophenol blue and 25% glycerol. DNA

samples were then electrophoresed on a 0.8% agarose gel at 60 V for 1 h with a running buffer of TAE (Tris-acetate-EDTA). Gels were stained for 30 min in an aqueous solution of ethidium bromide (0.5 μg/mL). DNA bands were visualized by transillumination with UV light and quantitated using AlphaImager^{TM} (Alpha Innotech Corporation). DNA topo IIα inhibitory activities of compounds were measured as follows. The mixture of 100 ng of supercoiled pBR322 plasmid DNA (Fermentas, USA) and 1 unit of human DNA topo IIα (Usb Corp., USA) were incubated with and without the prepared compounds in the assay buffer (10 mM Tris-HCl pH 7.9) containing 50 mM NaCl, 5 mM $MgCl_2$, 1 mM EDTA, 1 mM ATP, and 15 μg/mL bovine serum albumin) for 30 min at 37 °C. The reaction in a final volume of 10 μL was terminated by the addition of 3 μL of 7 mM EDTA. Reaction products were analyzed as in the DNA topo I mediated relaxation assay *in vitro*.

Cell viability assay.

To measure the anti-proliferative activity of the candidate compounds in various cancer cell lines, cell viability was assessed by measuring mitochondrial dehydrogenase activity with a Cell Counting Kit (CCK-8) purchased from Dojindo Laboratories (Japan). HCT15 (human colon cancer cell), BT474 (human breast cancer cell line) and T47D (a human HER2 negative breast cancer cell line) were purchased from the Korean Cell Line Bank. BT474, T47D and HCT15 were grown in RPMI 1640 medium (Welgene, Korea) in humidified 5% CO_2 incubator kept at 37 °C [82]. Each medium was supplemented with 10% fetal bovine serum (FBS) (HyClone, USA) and 1% penicillin (Sigma, USA). All media were changed every 2~3 days. Each cell line was seeded in 96-well plates in a density of 10^4 cells per well, incubated at 37 ℃ for 24 h and treated with compounds for 72 h. CCK-8 (10 μL) was added to each well.

After another 4 h of incubation at 37 °C, absorbance was measured at 450 nm using an ELISA Microplate Reader (VersaMax, Molecular Devices). To determine the IC_{50} values, the absorbance reading at 450 nm was fitted to the four-parameter logistic equation. The compounds of Adriamycin, Etoposide, and Camptothecin were purchased from Sigma (USA) and used as positive controls.

Molecular docking study.

The crystal structure of the ATPase domain of human Topo IIα complexed with AMP-PNP was retrieved from the Brookhaven Protein Data Bank (PDB entry 1ZXM). The water molecules and the ligand were removed and the hydrogen atoms were added using the software package Sybyl-X-2.0 (Tripos Associates Inc., St. Louis, MO). The coordinates for compounds **5a-i** were prepared and minimized energetically using a Tripos force field with Gasteiger-Huckel charges. The receptor and ligand file were prepared according to the original publication protocols [83]. Docking was carried out with simulations using the Lamarckian Genetic Algorithm. Default search parameters were used except for a population size of 270,000 and 50 docking runs. Finally, the docking was analyzed by clustering the orientations lying within 2.0 Å in the root-mean square deviation (rmsd) tolerance of each other to see the most favorable docking mode.

ATP competition assay and ATPase assay.

ATP competition assay was performed same as DNA topo II inhibition assay but with different ATP concentrations. The concentrations of ATP used were 1 mM and 2 mM. Etoposide was used as the positive control. Also, the DNA-dependent ATPase activity of human topo IIα was monitored using a slight modification of the method reported

elsewhere with a malachite green phosphate assay kit (Gentaur, Belgium) [84, 85]. Human topo IIα 0.1 unit and supercoiled pUC18 3.4 nM were incubated in a reaction buffer containing 10 mM Tris-Cl (pH 7.5), 175 mM KCl, 0.1 mM EDTA, 5 mM $MgCl_2$, 2 mM DTT, and 2.5% glycerol at 37 °C for 30 min in the presence or absence of 400 μM of compounds or novobiocin. The reaction was initiated by adding 400 μM ATP (Sigma, USA) and incubated for 30 min at 37 °C. The volume of the reaction solution after the addition of ATP was 80 μL. 20 μL of reagent A and B mixture (A:B ratio of 100:1), which was provided by the malachite green phosphate assay kit, was added to the reaction solution. The absorption of the reaction solution was read at 620 nm using a VERSAmax microplate reader (Molecular Devices, USA). The OD value was determined by the amount of inorganic phosphate complexed with malachite green and acidic molybdate. The inorganic phosphate is the product released from ATP hydrolysis performed by human topo IIα. The blank OD value was < 0.1 showing that no inorganic phosphate existed before ATP hydrolysis. The % inhibition of ATP hydrolysis was calculated by setting the control without the compound as 0% inhibition. Novobiocin was used as the positive control.

DNA-topo IIα cleavable complex assay.

A cleavage complex assay was carried out by the method previously reported with minor modifications. In brief, 125 ng supercoiled DNA pBR322 (Fermentas, USA), used as the substrate, was pre-incubated with 3 units of human DNA topo IIα (USB, USA) for 10 min, and then each compound was added and incubated at 37 °C for additional 20 min in a total of 10 μL reaction volume. The reaction was stopped with 1 μL of 10% SDS, followed by digestion with proteinase K and further incubated for 30 min at 45 °C. After the addition of the loading buffer, the reaction was heated for 2

min at 70 °C. Electrophoresis was carried out in a 0.8% agarose gel containing 0.5 μg/mL ethidium bromide in TAE buffer, and the gel was destained with distilled water for 20 min. DNA bands were visualized by transillumination with UV light and quantitated using AlphaImager^{TM} (Alpha Innotech Corporation).

Endogenous topo inhibition assay.

To assess the ability of compound **5d** to inhibit the function of topo activity in cells, HCT cells were treated with 50 and 100 μM of compound **5d** for 24 h and harvested. The nuclear lysate of each cell line was prepared according to the protocol provided by the manufacturer using the nuclear/cytosol fraction kit (BioVision, USA). The protein concentration in each nuclear extract was measured by Bradford assay. The topo reaction was performed with 100 μg protein of nuclear lysate, 100 ng pBR322 plasmid as a substrate and 1 × reaction buffer (200 mM Tris-Cl, pH 7.5, 100 mM $MgCl_2$, 10 mM ATP, 10mM EDTA, 10 mM dithiothreitol, 1.5 mM KCl and 300 μg/mL bovine serum albumin). The final reaction volume in each tube was kept equal, and the tubes were incubated at 37 °C for 30 min. Similar treatment was also done with a control plasmid of pBR322 containing no lysate to check the effect of the reaction buffer. After incubation, a fixed amount of all the samples was loaded on 0.9% horizontal agarose gel electrophoresis containing ethidium bromide. Gel was run for 4-5 h at 15-20 V. The result was visualized and quantified using AlphaImager^{TM} (Alpha Innotech Corporation).

Acknowledgements

This research was supported by the Basic Science Research Program through the National Research Foundation of Korea (NRF) funded by the Ministry of Education, Science and Technology (NRF-2013R1A1A2060408) and by a grant of the Korean Health Technology R&D Project, Ministry of Health & Welfare, Republic of Korea (HI14C2469).

References

[1] M.J. Meyers, G.B. Arhancet, S.L. Hockerman, X. Chen, S.A. Long, M.W. Mahoney, J.R. Rico, D.J. Garland, J.R. Blinn, J.T. Collins, S. Yang, H.-C. Huang, K.F. McGee, J.M. Wendling, J.D. Dietz, M.A. Payne, B.L. Homer, M.I. Heron, D.B. Reitz, X. Hu, Discovery of (3S,3aR)-2-(3-Chloro-4-cyanophenyl)-3-cyclopentyl-3,3a,4,5-tetrahydro-2H-benzo[g]indazole-7-carboxylic Acid (PF-3882845), an Orally Efficacious Mineralocorticoid Receptor (MR) Antagonist for Hypertension and Nephropathy, Journal of Medicinal Chemistry, 53 (2010) 5979-6002.

[2] J.H.M. Lange, M.A.W. van der Neut, A.P. den Hartog, H.C. Wals, J. Hoogendoorn, H.H. van Stuivenberg, B.J. van Vliet, C.G. Kruse, Synthesis, SAR and intramolecular hydrogen bonding pattern of 1,3,5-trisubstituted 4,5-dihydropyrazoles as potent cannabinoid CB1 receptor antagonists, Bioorganic & Medicinal Chemistry Letters, 20 (2010) 1752-1757.

[3] R.J. Chorvat, Peripherally restricted CB1 receptor blockers, Bioorganic & Medicinal Chemistry Letters, 23 (2013) 4751-4760.

[4] M. Atobe, K. Naganuma, M. Kawanishi, A. Morimoto, K.-i. Kasahara, S. Ohashi, H. Suzuki, T. Hayashi, S. Miyoshi, SAR-based optimization of 2-(1H-pyrazol-1-yl)-thiazole derivatives as highly potent EP1 receptor antagonists, Bioorganic & Medicinal Chemistry Letters, 23 (2013) 6569-6576.

[5] N. Gökhan-Kelekçi, S. Yabanoğlu, E. Küpeli, U. Salgın, Ö. Özgen, G. Uçar, E. Yeşilada, E. Kendi, A. Yeşilada, A.A. Bilgin, A new therapeutic approach in Alzheimer disease: Some novel

pyrazole derivatives as dual MAO-B inhibitors and antiinflammatory analgesics, Bioorganic & Medicinal Chemistry, 15 (2007) 5775-5786.

[6] N. Mishra, D. Sasmal, Development of selective and reversible pyrazoline based MAO-B inhibitors: Virtual screening, synthesis and biological evaluation, Bioorganic & Medicinal Chemistry Letters, 21 (2011) 1969-1973.

[7] M. Jagrat, J. Behera, S. Yabanoglu, A. Ercan, G. Ucar, B.N. Sinha, V. Sankaran, A. Basu, V. Jayaprakash, Pyrazoline based MAO inhibitors: Synthesis, biological evaluation and SAR studies, Bioorganic & Medicinal Chemistry Letters, 21 (2011) 4296-4300.

[8] F. Chimenti, S. Carradori, D. Secci, A. Bolasco, B. Bizzarri, P. Chimenti, A. Granese, M. Yáñez, F. Orallo, Synthesis and inhibitory activity against human monoamine oxidase of N1-thiocarbamoyl-3,5-di(hetero)aryl-4,5-dihydro-(1H)-pyrazole derivatives, European Journal of Medicinal Chemistry, 45 (2010) 800-804.

[9] E. Maccioni, S. Alcaro, F. Orallo, M.C. Cardia, S. Distinto, G. Costa, M. Yanez, M.L. Sanna, S. Vigo, R. Meleddu, D. Secci, Synthesis of new 3-aryl-4,5-dihydropyrazole-1-carbothioamide derivatives. An investigation on their ability to inhibit monoamine oxidase, European Journal of Medicinal Chemistry, 45 (2010) 4490-4498.

[10] K. Nepali, G. Singh, A. Turan, A. Agarwal, S. Sapra, R. Kumar, U.C. Banerjee, P.K. Verma, N.K. Satti, M.K. Gupta, O.P. Suri, K.L. Dhar, A rational approach for the design and synthesis of 1-acetyl-3,5-diaryl-4,5-dihydro(1H)pyrazoles as a new class of potential non-purine xanthine oxidase inhibitors, Bioorganic & Medicinal Chemistry, 19 (2011) 1950-1958.

[11] T.-S. Jeong, K. Soon Kim, J.-R. Kim, K.-H. Cho, S. Lee, W. Song Lee, Novel 3,5-diaryl pyrazolines and pyrazole as low-density lipoprotein (LDL) oxidation inhibitor, Bioorganic & Medicinal Chemistry Letters, 14 (2004) 2719-2723.

[12] G. Wanare, R. Aher, N. Kawathekar, R. Ranjan, N.K. Kaushik, D. Sahal, Synthesis of novel α-pyranochalcones and pyrazoline derivatives as Plasmodium falciparum growth inhibitors, Bioorganic & Medicinal Chemistry Letters, 20 (2010) 4675-4678.

[13] C. Blackburn, M.O. Duffey, A.E. Gould, B. Kulkarni, J.X. Liu, S. Menon, M. Nagayoshi, T.J. Vos, J. Williams, Discovery and optimization of N-acyl and N-aroylpyrazolines as B-Raf kinase inhibitors, Bioorganic & Medicinal Chemistry Letters, 20 (2010) 4795-4799.

[14] M.O. Duffey, R. Adams, C. Blackburn, R.W. Chau, S. Chen, K.M. Galvin, K. Garcia, A.E. Gould, P.D. Greenspan, S. Harrison, S.-C. Huang, M.-S. Kim, B. Kulkarni, S. Langston, J.X. Liu, L.-T. Ma, S. Menon, M. Nagayoshi, R.S. Rowland, T.J. Vos, T. Xu, J.J. Yang, S. Yu, Q. Zhang, Discovery and optimization of pyrazoline compounds as B-Raf inhibitors, Bioorganic & Medicinal Chemistry Letters, 20 (2010) 4800-4804.

[15] F.F. Barsoum, A.S. Girgis, Facile synthesis of bis(4,5-dihydro-1H-pyrazole-1-carboxamides) and their thio-analogues of potential PGE2 inhibitory properties, European Journal of Medicinal Chemistry, 44 (2009) 2172-2177.

[16] L. Gomez, J.G. Breitenbucher, PDE2 inhibition: Potential for the treatment of cognitive disorders, Bioorganic & Medicinal Chemistry Letters, 23 (2013) 6522-6527.

[17] R. Tripathy, R.J. McHugh, A.K. Ghose, G.R. Ott, T.S. Angeles, M.S. Albom, Z. Huang, L.D. Aimone, M. Cheng, B.D. Dorsey, Pyrazolone-based anaplastic lymphoma kinase (ALK) inhibitors: Control of selectivity by a benzyloxy group, Bioorganic & Medicinal Chemistry Letters, 21 (2011) 7261-7264.

[18] K. Ngu, D.S. Weinstein, W. Liu, C. Langevine, D.W. Combs, S. Zhuang, X. Chen, C.S. Madsen, T.W. Harper, S. Ahmad, J.A. Robl, Pyrazole-based sulfonamide and sulfamides as potent inhibitors of mammalian 15-lipoxygenase, Bioorganic & Medicinal Chemistry Letters, 21 (2011) 4141-4145.

[19] Z.A. Kaplancikli, G. Turan-Zitouni, A. Özdemir, Ö. Devrim Can, P. Chevallet, Synthesis and antinociceptive activities of some pyrazoline derivatives, European Journal of Medicinal Chemistry, 44 (2009) 2606-2610.

[20] N. Jagerovic, C. Cano, J. Elguero, P. Goya, L.F. Callado, J. Javier Meana, R.o. Girón, R. Abalo, D. Ruiz, C. Goicoechea, M. Isabel Martín, Long-Acting Fentanyl Analogues: Synthesis

and Pharmacology of N-(1-Phenylpyrazolyl)-N-(1-phenylalkyl-4-piperidyl)propanamides, Bioorganic & Medicinal Chemistry, 10 (2002) 817-827.

[21] S.A.F. Rostom, Synthesis and in vitro antitumor evaluation of some indeno[1,2-c]pyrazol(in)es substituted with sulfonamide, sulfonylurea(-thiourea) pharmacophores, and some derived thiazole ring systems, Bioorganic & Medicinal Chemistry, 14 (2006) 6475-6485.

[22] C. Congiu, V. Onnis, L. Vesci, M. Castorina, C. Pisano, Synthesis and in vitro antitumor activity of new 4,5-dihydropyrazole derivatives, Bioorganic & Medicinal Chemistry, 18 (2010) 6238-6248.

[23] R.S. Joshi, P.G. Mandhane, S.D. Diwakar, S.K. Dabhade, C.H. Gill, Synthesis, analgesic and anti-inflammatory activities of some novel pyrazolines derivatives, Bioorganic & Medicinal Chemistry Letters, 20 (2010) 3721-3725.

[24] R. Bashir, S. Ovais, S. Yaseen, H. Hamid, M.S. Alam, M. Samim, S. Singh, K. Javed, Synthesis of some new 1,3,5-trisubstituted pyrazolines bearing benzene sulfonamide as anticancer and anti-inflammatory agents, Bioorganic & Medicinal Chemistry Letters, 21 (2011) 4301-4305.

[25] O.I. El-Sabbagh, M.M. Baraka, S.M. Ibrahim, C. Pannecouque, G. Andrei, R. Snoeck, J. Balzarini, A.A. Rashad, Synthesis and antiviral activity of new pyrazole and thiazole derivatives, European Journal of Medicinal Chemistry, 44 (2009) 3746-3753.

[26] Z. Özdemir, H.B. Kandilci, B. Gümüşel, Ü. Çalış, A.A. Bilgin, Synthesis and studies on antidepressant and anticonvulsant activities of some 3-(2-furyl)-pyrazoline derivatives, European Journal of Medicinal Chemistry, 42 (2007) 373-379.

[27] N.D. Amnerkar, K.P. Bhusari, Synthesis, anticonvulsant activity and 3D-QSAR study of some prop-2-eneamido and 1-acetyl-pyrazolin derivatives of aminobenzothiazole, European Journal of Medicinal Chemistry, 45 (2010) 149-159.

[28] S. Bhandari, A. Tripathi, S. Saraf, Novel 2-pyrazoline derivatives as potential anticonvulsant agents, Medicinal Chemistry Research, 22 (2013) 5290-5296.

[29] Z.A. Kaplancıklı, A. Özdemir, G. Turan-Zitouni, M.D. Altıntop, Ö.D. Can, New pyrazoline derivatives and their antidepressant activity, European Journal of Medicinal Chemistry, 45 (2010) 4383-4387.

[30] K. Manna, Y.K. Agrawal, Design, synthesis, and antitubercular evaluation of novel series of 3-benzofuran-5-aryl-1-pyrazolyl-pyridylmethanone and 3-benzofuran-5-aryl-1-pyrazolylcarbonyl-4-oxo-naphthyridin analogs, European Journal of Medicinal Chemistry, 45 (2010) 3831-3839.

[31] M.J. Ahsan, J.G. Samy, H. Khalilullah, M.S. Nomani, P. Saraswat, R. Gaur, A. Singh, Molecular properties prediction and synthesis of novel 1,3,4-oxadiazole analogues as potent antimicrobial and antitubercular agents, Bioorganic & Medicinal Chemistry Letters, 21 (2011) 7246-7250.

[32] B.N. Acharya, D. Saraswat, M. Tiwari, A.K. Shrivastava, R. Ghorpade, S. Bapna, M.P. Kaushik, Synthesis and antimalarial evaluation of 1, 3, 5-trisubstituted pyrazolines, European Journal of Medicinal Chemistry, 45 (2010) 430-438.

[33] W.-K. Choi, M.I. El-Gamal, H.S. Choi, D. Baek, C.-H. Oh, New diarylureas and diarylamides containing 1,3,4-triarylpyrazole scaffold: Synthesis, antiproliferative evaluation against melanoma cell lines, ERK kinase inhibition, and molecular docking studies, European Journal of Medicinal Chemistry, 46 (2011) 5754-5762.

[34] A. Budakoti, A.R. Bhat, A. Azam, Synthesis of new 2-(5-substituted-3-phenyl-2-pyrazolinyl)-1,3-thiazolino[5,4-b]quinoxaline derivatives and evaluation of their antiamoebic activity, European Journal of Medicinal Chemistry, 44 (2009) 1317-1325.

[35] A. Budakoti, M. Abid, A. Azam, Synthesis and antiamoebic activity of new 1-N-substituted thiocarbamoyl-3,5-diphenyl-2-pyrazoline derivatives and their Pd(II) complexes, European Journal of Medicinal Chemistry, 41 (2006) 63-70.

[36] A. Budakoti, M. Abid, A. Azam, Syntheses, characterization and in vitro antiamoebic activity of new Pd(II) complexes with 1-N-substituted thiocarbamoyl-3,5-diphenyl-2-pyrazoline derivatives, European Journal of Medicinal Chemistry, 42 (2007) 544-551.

[37] M. Abid, A.R. Bhat, F. Athar, A. Azam, Synthesis, spectral studies and antiamoebic activity of new 1-N-substituted thiocarbamoyl-3-phenyl-2-pyrazolines, European Journal of Medicinal Chemistry, 44 (2009) 417-425.

[38] F. Hayat, A. Salahuddin, S. Umar, A. Azam, Synthesis, characterization, antiamoebic activity and cytotoxicity of novel series of pyrazoline derivatives bearing quinoline tail, European Journal of Medicinal Chemistry, 45 (2010) 4669-4675.

[39] K. Manna, Y.K. Agrawal, Microwave assisted synthesis of new indophenazine 1,3,5-trisubstruted pyrazoline derivatives of benzofuran and their antimicrobial activity, Bioorganic & Medicinal Chemistry Letters, 19 (2009) 2688-2692.

[40] P.-L. Zhao, F. Wang, M.-Z. Zhang, Z.-M. Liu, W. Huang, G.-F. Yang, Synthesis, Fungicidal, and Insecticidal Activities of β-Methoxyacrylate-Containing N-Acetyl Pyrazoline Derivatives, Journal of Agricultural and Food Chemistry, 56 (2008) 10767-10773.

[41] H. Khalilullah, S. Khan, M.J. Ahsan, B. Ahmed, Synthesis and antihepatotoxic activity of 5-(2,3-dihydro-1,4-benzodioxane-6-yl)-3-substituted-phenyl-4,5-dihydro-1H-pyrazole derivatives, Bioorganic & Medicinal Chemistry Letters, 21 (2011) 7251-7254.

[42] D. Havrylyuk, B. Zimenkovsky, O. Vasylenko, L. Zaprutko, A. Gzella, R. Lesyk, Synthesis of novel thiazolone-based compounds containing pyrazoline moiety and evaluation of their anticancer activity, European Journal of Medicinal Chemistry, 44 (2009) 1396-1404.

[43] S.-Q. Wang, Q.-H. Wu, H.-Y. Wang, X.-X. Zheng, S.-L. Shen, Y.-R. Zhang, J.-Y. Miao, B.-X. Zhao, A novel pyrazoline-based selective fluorescent probe for detecting reduced glutathione and its application in living cells and serum, Analyst, 138 (2013) 7169-7174.

[44] P. McCormack, Celecoxib, Drugs, 71 (2011) 2457-2489.

[45] S.P. Society, 17th ed., Amer Pharmaceutical Assn2000.

[46] S.P. Macmillan, A combination for treating cold and cough, Google Patents, 2003.

[47] M. Underwood, Diagnosis and management of gout, BMJ, 332 (2006) 1315-1319.

[48] U. Trstenjak, J. Ilas, D. Kikelj, Transformation of a selective factor Xa inhibitor rivaroxaban into a dual factor Xa/thrombin inhibitor by modification of the morpholin-3-one moiety, MedChemComm, 5 (2014) 197-202.

[49] P. Pacher, A. Nivorozhkin, C. SzabÓ, Therapeutic Effects of Xanthine Oxidase Inhibitors: Renaissance Half a Century after the Discovery of Allopurinol, Pharmacological reviews, 58 (2006) 87-114.

[50] T.M. Fong, S.B. Heymsfield, Cannabinoid-1 receptor inverse agonists: current understanding of mechanism of action and unanswered questions, Int J Obes, 33 (2009) 947-955.

[51] R.A. Mesa, U. Yasothan, P. Kirkpatrick, Ruxolitinib, Nat Rev Drug Discov, 11 (2012) 103-104.

[52] S.G. Browne, Trial of a long-acting sulfonamide sulfaphenazole (Orisul, Ciba), in the treatment of leprosy, Int J Lepr, 29 (1961) 502-505.

[53] K. Brune, The early history of non-opioid analgesics, Acute Pain, 1 (1997) 33-40.

[54] N.M.W.J. de Bruin, J. Prickaerts, J.H.M. Lange, S. Akkerman, E. Andriambeloson, M. de Haan, J. Wijnen, M. van Drimmelen, E. Hissink, L. Heijink, C.G. Kruse, SLV330, a cannabinoid CB1 receptor antagonist, ameliorates deficits in the T-maze, object recognition and Social Recognition Tasks in rodents, Neurobiology of Learning and Memory, 93 (2010) 522-531.

[55] B.N.M.W.J. de, J.H.M. Lange, C.G. Kruse, A.H. Herremans, A.N.M. Schoffelmeer, D.M. van, V.T.J. De, SLV330, a cannabinoid CB(1) receptor antagonist, attenuates ethanol and nicotine seeking and improves inhibitory response control in rats, Behav Brain Res, 217 (2011) 408-415.

[56] M.A. Iniguez, C. Punzon, C. Cacheiro-Llaguno, M.D. Diaz-Munoz, J. Duque, R. Cuberes, I. Alvarez, E.M. Andres, J. Buxens, H. Buschmann, J.M. Vela, M. Fresno, Cyclooxygenase-

independent inhibitory effects on T cell activation of novel 4,5-dihydro-3 trifluoromethyl pyrazole cyclooxygenase-2 inhibitors, Int. Immunopharmacol., 10 (2010) 1295-1304.

[57] M. Wagemakers, d.W.G.E. van, R. Cuberes, I. Alvarez, E.M. Andres, J. Buxens, J.M. Vela, H. Moorlag, J.J.A. Mooij, G. Molema, COX-2 Inhibition Combined with Radiation Reduces Orthotopic Glioma Outgrowth by Targeting the Tumor Vasculature, Transl Oncol, 2 (2009) 1-7.

[58] A.F.M.M. Rahman, S.-E. Park, A.A. Kadi, Y. Kwon, Fluorescein Hydrazones as Novel Nonintercalative Topoisomerase Catalytic Inhibitors with Low DNA Toxicity, J. Med. Chem., 57 (2014) 9139-9151.

[59] S.-E. Park, I.-H. Chang, K.-Y. Jun, E. Lee, E.-S. Lee, Y. Na, Y. Kwon, 3-(3-Butylamino-2-hydroxy-propoxy)-1-hydroxy-xanthen-9-one acts as a topoisomerase IIα catalytic inhibitor with low DNA damage, European Journal of Medicinal Chemistry, 69 (2013) 139-145.

[60] U. Thapa, P. Thapa, R. Karki, M. Yun, J.H. Choi, Y. Jahng, E. Lee, K.-H. Jeon, Y. Na, E.-M. Ha, W.-J. Cho, Y. Kwon, E.-S. Lee, Synthesis of 2,4-diaryl chromenopyridines and evaluation of their topoisomerase I and II inhibitory activity, cytotoxicity, and structure–activity relationship, European Journal of Medicinal Chemistry, 46 (2011) 3201-3209.

[61] K.-Y. Jun, E.-Y. Lee, M.-J. Jung, O.-H. Lee, E.-S. Lee, H.-Y. Park Choo, Y. Na, Y. Kwon, Synthesis, biological evaluation, and molecular docking study of 3-(3′-heteroatom substituted-2′-hydroxy-1′-propyloxy) xanthone analogues as novel topoisomerase IIα catalytic inhibitor, European Journal of Medicinal Chemistry, 46 (2011) 1964-1971.

[62] P. Thapa, K.-Y. Jun, T.M. Kadayat, C. Park, Z. Zheng, T.B. Thapa Magar, G. Bist, A. Shrestha, Y. Na, Y. Kwon, E.-S. Lee, Design and synthesis of conformationally constrained hydroxylated 4-phenyl-2-aryl chromenopyridines as novel and selective topoisomerase II-targeted antiproliferative agents, Bioorganic & Medicinal Chemistry, 23 (2015) 6454-6466.

[63] R. Karki, C. Park, K.-Y. Jun, J.-G. Jee, J.-H. Lee, P. Thapa, T.M. Kadayat, Y. Kwon, E.-S. Lee, Synthesis, antitumor activity, and structure–activity relationship study of trihydroxylated

2,4,6-triphenyl pyridines as potent and selective topoisomerase II inhibitors, European Journal of Medicinal Chemistry, 84 (2014) 555-565.

[64] K.-Y. Jun, H. Kwon, S.-E. Park, E. Lee, R. Karki, P. Thapa, J.-H. Lee, E.-S. Lee, Y. Kwon, Discovery of dihydroxylated 2,4-diphenyl-6-thiophen-2-yl-pyridine as a non-intercalative DNA-binding topoisomerase II-specific catalytic inhibitor, European Journal of Medicinal Chemistry, 80 (2014) 428-438.

[65] P. Thapa, R. Karki, M. Yun, T.M. Kadayat, E. Lee, H.B. Kwon, Y. Na, W.-J. Cho, N.D. Kim, B.-S. Jeong, Y. Kwon, E.-S. Lee, Design, synthesis, and antitumor evaluation of 2,4,6-triaryl pyridines containing chlorophenyl and phenolic moiety, European Journal of Medicinal Chemistry, 52 (2012) 123-136.

[66] P. Thapa, R. Karki, H.Y. Yoo, P.-H. Park, E. Lee, K.-H. Jeon, Y. Na, W.-J. Cho, Y. Kwon, E.-S. Lee, 2,4-Diaryl-5,6-dihydro-1,10-phenanthroline and 2,4-diaryl-5,6-dihydrothieno[2,3-h] quinoline derivatives for topoisomerase I and II inhibitory activity, cytotoxicity, and structure–activity relationship study, Bioorganic Chemistry, 40 (2012) 67-78.

[67] Y.-J. Qin, Y.-j. Li, A.-Q. Jiang, M.-R. Yang, Q.-Z. Zhu, H. Dong, H.-L. Zhu, Design, synthesis and biological evaluation of novel pyrazoline-containing derivatives as potential tubulin assembling inhibitors, European Journal of Medicinal Chemistry, 94 (2015) 447-457.

[68] A.M. Rahman, M.W. Attwa, P. Ahmad, M. Baseeruddin, A.A. Kadi, Fragmentation Behavior Studies of Chalcones Employing Direct Analysis in Real Time (DART), Mass Spectrometry Letters, 4 (2013) 30-33.

[69] S.G. Kini, A.R. Bhat, B. Bryant, J.S. Williamson, F.E. Dayan, Synthesis, antitubercular activity and docking study of novel cyclic azole substituted diphenyl ether derivatives, European Journal of Medicinal Chemistry, 44 (2009) 492-500.

[70] S.M. Vos, E.M. Tretter, B.H. Schmidt, J.M. Berger, All tangled up: how cells direct, manage and exploit topoisomerase function, Nature reviews. Molecular cell biology, 12 (2011) 827-841.

[71] J.L. Nitiss, Targeting DNA topoisomerase II in cancer chemotherapy, Nat Rev Cancer, 9 (2009) 338-350.

[72] H. Wei, A.J. Ruthenburg, S.K. Bechis, G.L. Verdine, Nucleotide-dependent Domain Movement in the ATPase Domain of a Human Type IIA DNA Topoisomerase, Journal of Biological Chemistry, 280 (2005) 37041-37047.

[73] M.J. Robinson, A.H. Corbett, N. Osheroff, Effects of topoisomerase II-targeted drugs on enzyme-mediated DNA cleavage and ATP hydrolysis: Evidence for distinct drug interaction domains on topoisomerase II, Biochemistry, 32 (1993) 3638-3643.

[74] M. Sehested, P.B. Jensen, Mapping of DNA topoisomerase II poisons (etoposide, clerocidin) and catalytic inhibitors (aclarubicin, ICRF-187) to four distinct steps in the topoisomerase II catalytic cycle, Biochemical Pharmacology, 51 (1996) 879-886.

[75] M.Y. Wani, A.R. Bhat, A. Azam, D.H. Lee, I. Choi, F. Athar, Synthesis and in vitro evaluation of novel tetrazole embedded 1,3,5-trisubstituted pyrazoline derivatives as Entamoeba histolytica growth inhibitors, European Journal of Medicinal Chemistry, 54 (2012) 845-854.

[76] S.M.K.P. Rao, Synthesis, characterization and antimicrobial activity of some chalcones, International journal of Pharmaceutical research and Development, 4 (2012) 97-101.

[77] J.B.-J. Teh, P.S. Patil, H.-K. Fun, I.A. Razak, S.M. Dharmaprakash, 1-(4-Chlorophenyl)-3-(2-furyl)prop-2-en-1-one, Acta Crystallographica Section E, 62 (2006) o2261-o2262.

[78] K. Kapoor, V.K. Gupta, R. Kant, J.R. Pandya, S.B. Lade, H.S. Joshi, (E)-3-(Furan-2-yl)-1-(4-methoxyphenyl)prop-2-en-1-one, Acta Crystallographica Section E, 67 (2011) o3185.

[79] D. Sriram, P. Yogeeswari, D.R.K. Vyas, P. Senthilkumar, P. Bhat, M. Srividya, 5-Nitro-2-furoic acid hydrazones: Design, synthesis and in vitro antimycobacterial evaluation against log and starved phase cultures, Bioorganic & Medicinal Chemistry Letters, 20 (2010) 4313-4316.

[80] E. Campaigne, R.L. Thompson, J.E. Van Werth, Some Heterocyclic Aldehyde Thiosemicarbazones Possing Anti-viral Activity, Journal of Medicinal and Pharmaceutical Chemistry, 1 (1959) 577-599.

[81] J.F. Riou, P. Fosse, H.N. Chi, A.K. Larsen, M.C. Bissery, L. Grondard, J.M. Saucier, E. Bisagni, F. Lavelle, Intoplicine (RP 60475) and its derivatives, a new class of antitumor agents inhibiting both topoisomerase I and II activities, Cancer Res., 53 (1993) 5987-5993.

[82] J. Seo, J.Y. Lee, M.-S. Sung, C.J. Byun, D.-H. Cho, H.-J. Lee, J.-H. Park, H.-S. Cho, S.-J. Cho, I. Jo, Arsenite Acutely Decreases Nitric Oxide Production via the ROS—Protein Phosphatase 1—Endothelial Nitric Oxide Synthase-Thr(497) Signaling Cascade, Biomolecules & Therapeutics, 22 (2014) 510-518.

[83] G.M. Morris, D.S. Goodsell, R.S. Halliday, R. Huey, W.E. Hart, R.K. Belew, A.J. Olson, Automated docking using a Lamarckian genetic algorithm and an empirical binding free energy function, Journal of Computational Chemistry, 19 (1998) 1639-1662.

[84] P. Chene, J. Rudloff, J. Schoepfer, P. Furet, P. Meier, Z. Qian, J.-M. Schlaeppi, R. Schmitz, T. Radimerski, Catalytic inhibition of topoisomerase II by a novel rationally designed ATP-competitive purine analogue, BMC Chemical Biology, 9 (2009) 1.

[85] P.A. Lanzetta, L.J. Alvarez, P.S. Reinach, O.A. Candia, An improved assay for nanomole amounts of inorganic phosphate, Analytical Biochemistry, 100 (1979) 95-97.

Graphical abstract

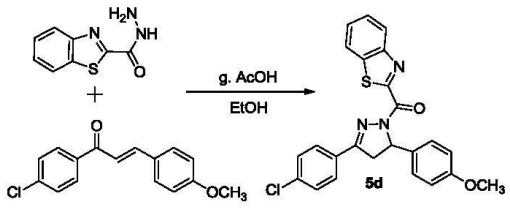

- Inhibited 90% topo IIα (Etoposide 96%)
- Functioned as ATP-competitive human topoisomerase IIα catalytic inhibitor.
- Inhibited endogenous topo 78.0% at 50μM (Etoposide 36.0% at 50μM)

Highlights

- Synthesis a series of pyrazoline derivatives
- ATP-competitive human topoisomerase IIα catalytic inhibitor
- Inhibited endogenous topo-mediated pBR322 plasmid relaxation more efficiently than Etoposide.